CULTURA MATEMATICA @ POLIMI
15 marzo 2017

# La matematica dei terremoti

Alfio Quarteroni

CMCS - EPFL (Lausanne)
MOX - Politecnico di Milano (on leave)

Jointly with:
Paola Antonietti, Ilario Mazzieri (MOX)

# Acknowledgments: The SPEED People

A. Quarteroni
EPFL & PoliMi

P. Antonietti
MOX, PoliMI

I. Mazzieri
MOX, PoliMI

R. Paolucci
DICA, PoliMI

M. Stupazzini
Munich RE

C. Smerzini
DICA, PoliMI

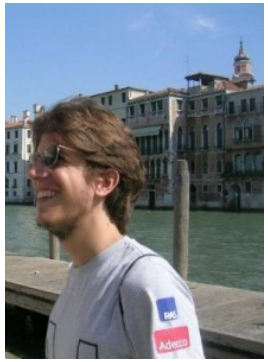

Filippo Gatti
DICA, PoliMI
Ecole Centrale
Paris Supélec

Ali Ozcebe
DICA, PoliMI

http://speed.mox.polimi.it


Other Contributors

Paride Dagna (Cineca), Paolo Ramieri (Cineca)
Carlo Marcati (UMPC, Paris VI, France), Niccolò Dal Santo (EPFL, Switzerland)
Roberto Guidotti (University of Illinois, US), Erika Schiappapietra (Dip. Protezione Civile)
Maria Infantino (DICA, Politecnico di Milano), Samuele Mauri (EPFL, Switzerland)
Antonio Nicolò (MOX, Politecnico di Milano), Alberto Ferroni (MOX, Politecnico di Milano)
Kiana Hashemi (DICA, Politecnico di Milano)

# Major Events and Losses in 2016

NatCatSERVICE

## Loss events worldwide 2016
## Geographical overview

Munich RE

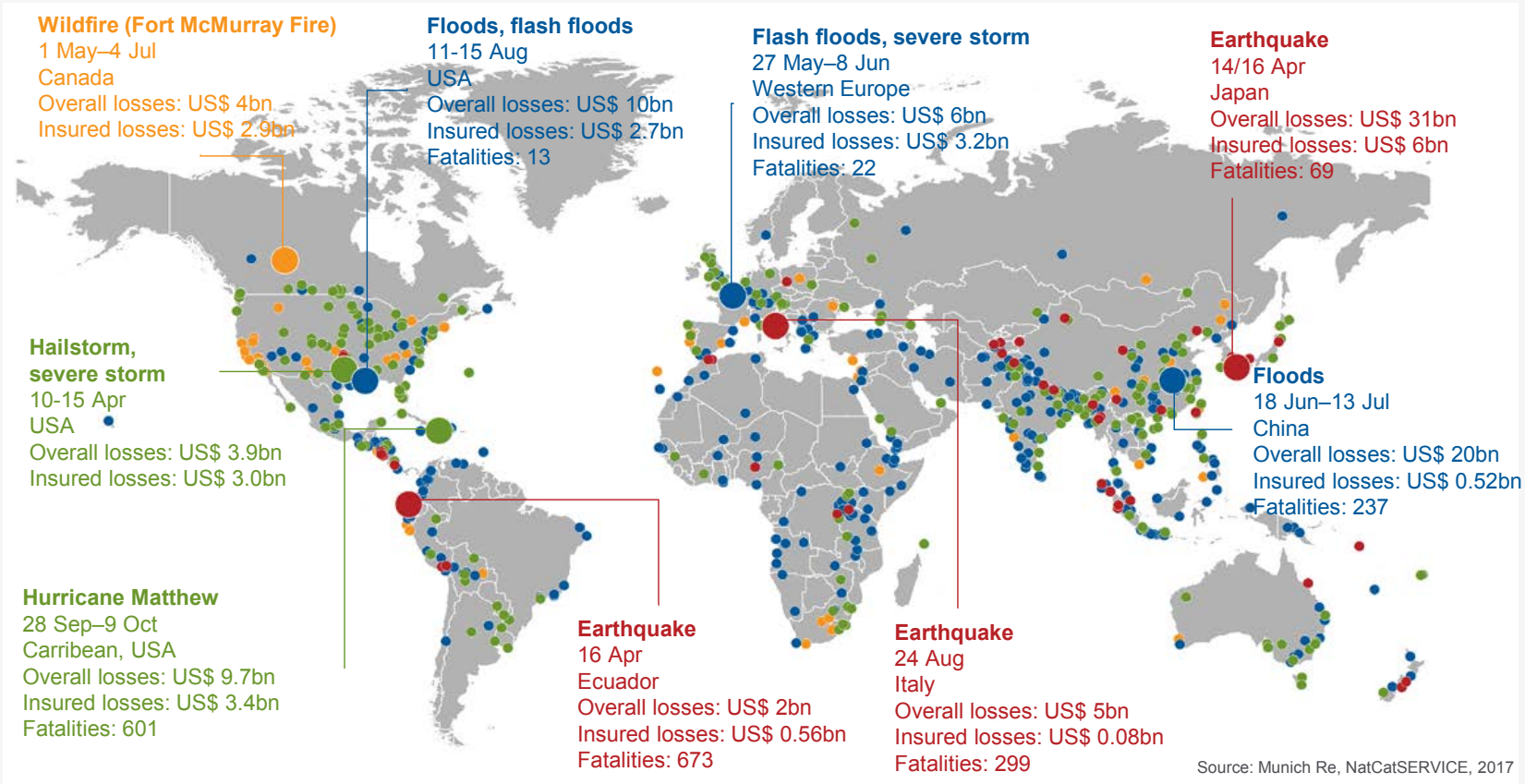


- **Geophysical events** (Earthquake, tsunami, volcanic activity)
- **Meteorological events** (Tropical storm, extratropical storm, convective storm, local storm)
- **Hydrological events** (Flood, mass movement)
- **Climatological events** (Extreme temperature, drought, wildfire)

- **Loss events**
- **Selection of catastrophes**

NatCatSERVICE

## Loss events worldwide 1980 – 2016

### Number of severe catastrophes by peril

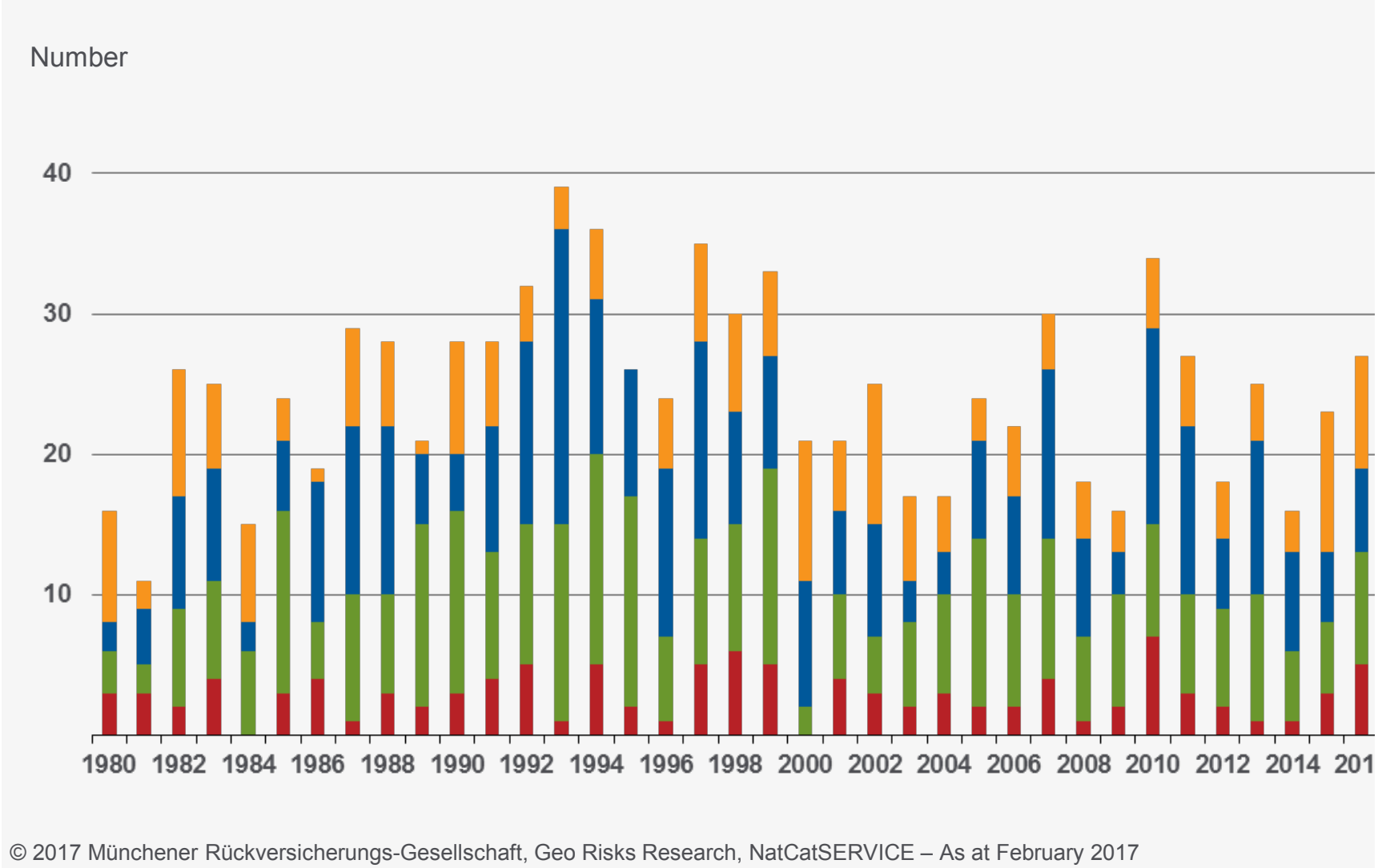

NatCatSERVICE

# Loss events worldwide 1980 – 2016
## Overall and insured losses

Munich RE

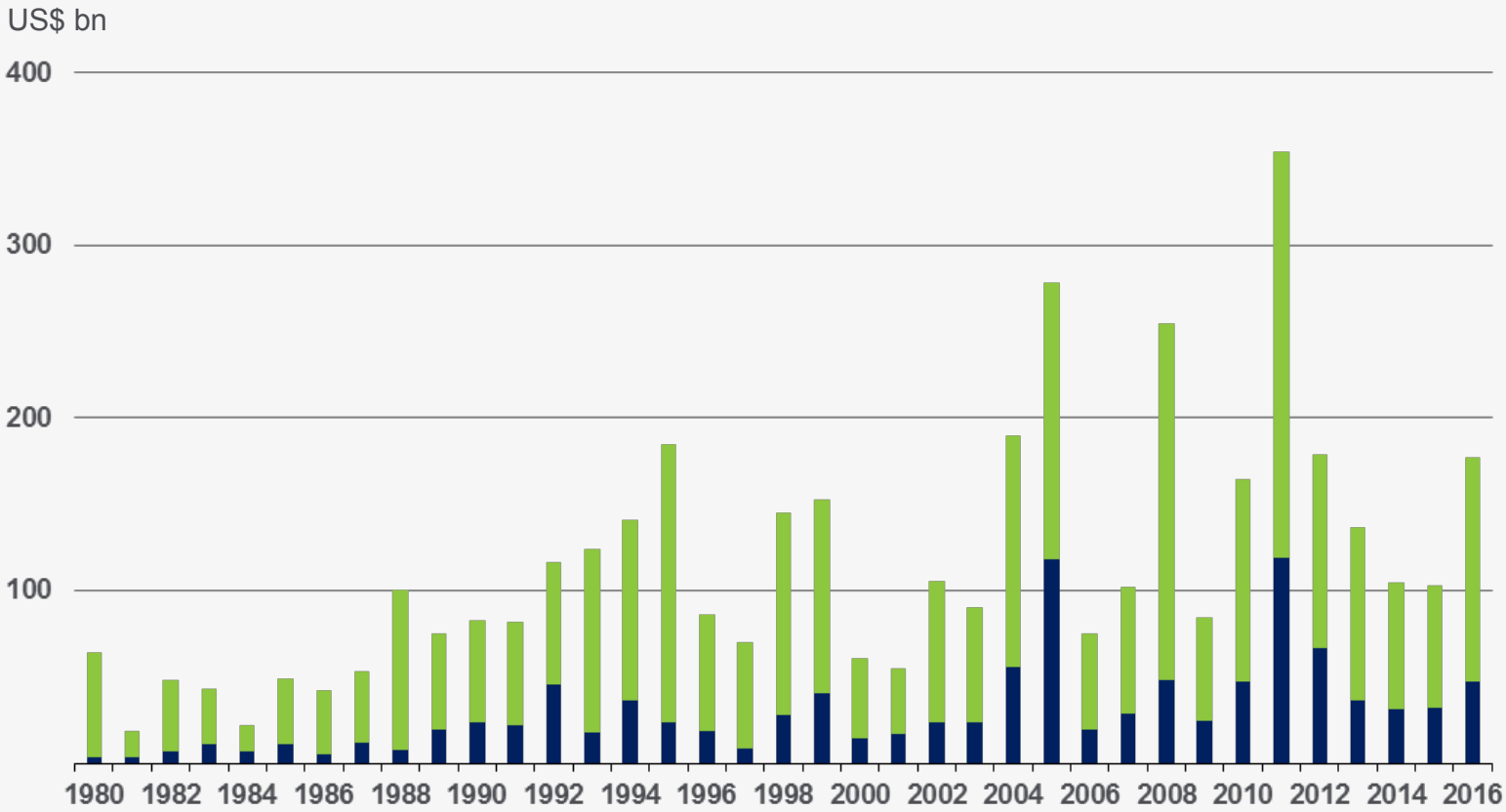


Inflation adjusted via country-specific consumer price index and consideration of exchange rate fluctuations between local currency and US$.

NatCatSERVICE

# Loss events worldwide 1980 – 2016
## Percentage distribution

Munich RE

### Number of relevant events: 16,500

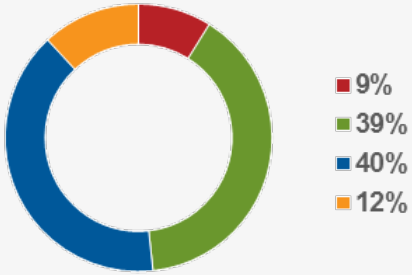


### Overall losses: US$ 4,200bn

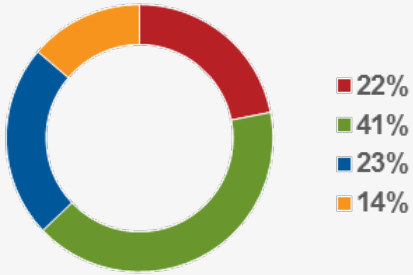


### Fatalities: 1,708,000

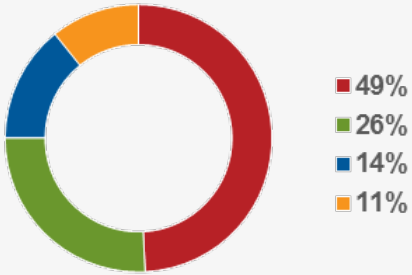


### Insured losses: US$ 1,100bn

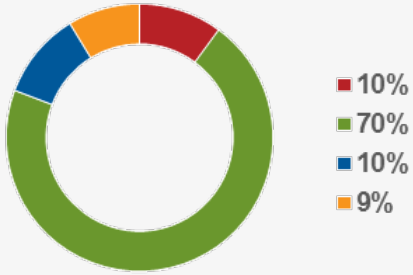


- **Geophysical events** (Earthquake, tsunami, volcanic activity)
- **Meteorological events** (Tropical storm, extratropical storm, convective storm, local storm)
- **Hydrological events** (Flood, mass movement)
- **Climatological events** (Extreme temperature, drought, forest fire)

Accounted events have caused at least one fatality and/or produced normalized losses ≥ US$ 100k, 300k, 1m, or 3m (depending on the assigned World Bank income group of the affected country).

Inflation adjusted via country-specific consumer price index and consideration of exchange rate fluctuations between local currency and US$.

NatCatSERVICE

# Significant loss events worldwide 1980 – 2016

## 10 deadliest events

Munich RE

| Date | Event | Affected area | Overall losses in US$ m original values | Insured losses in US$ m original values | Fatalities |
|---|---|---|---|---|---|
| 26.12.2004 | Earthquake, tsunami | Sri Lanka, Indonesia, Thailand, India, Bangladesh, Myanmar, Maldives, Malaysia | 10,000 | 1,000 | **220,000** |
| 12.1.2010 | Earthquake | Haiti | 8,000 | 200 | **159,000** |
| 2-5.5.2008 | Cyclone Nargis | Myanmar | 4,000 | | **140,000** |
| 29-30.4.1991 | Tropical cyclone | Bangladesh | 3,000 | 100 | **139,000** |
| 8.10.2005 | Earthquake | Pakistan, India, Afghanistan | 5,200 | 5 | **88,000** |
| 12.5.2008 | Earthquake | China | 85,000 | 300 | **84,000** |
| July - Aug 2003 | Heat wave | Europe | 14,000 | 1,100 | **70,000** |
| July - Sep 2010 | Heat wave | Russian Federation | | | **56,000** |
| 20.6.1990 | Earthquake | Iran | 7,100 | 100 | **40,000** |
| 26.12.2003 | Earthquake | Iran | 500 | 20 | **26,200** |

Source: Munich Re, NatCatSERVICE, 2017

# Geophysics of earthquakes in a nutshell

Un terremoto è liberazione di energia.

Scatena in poche decine di secondi l'energia accumulata in decenni o secoli in un dato volume della crosta terrestre.

E' una prova di vitalità della Terra e si origina quando la crosta terrestre si separa in due elementi che scivolano l'uno rispetto all'altro lungo un piano di faglia.

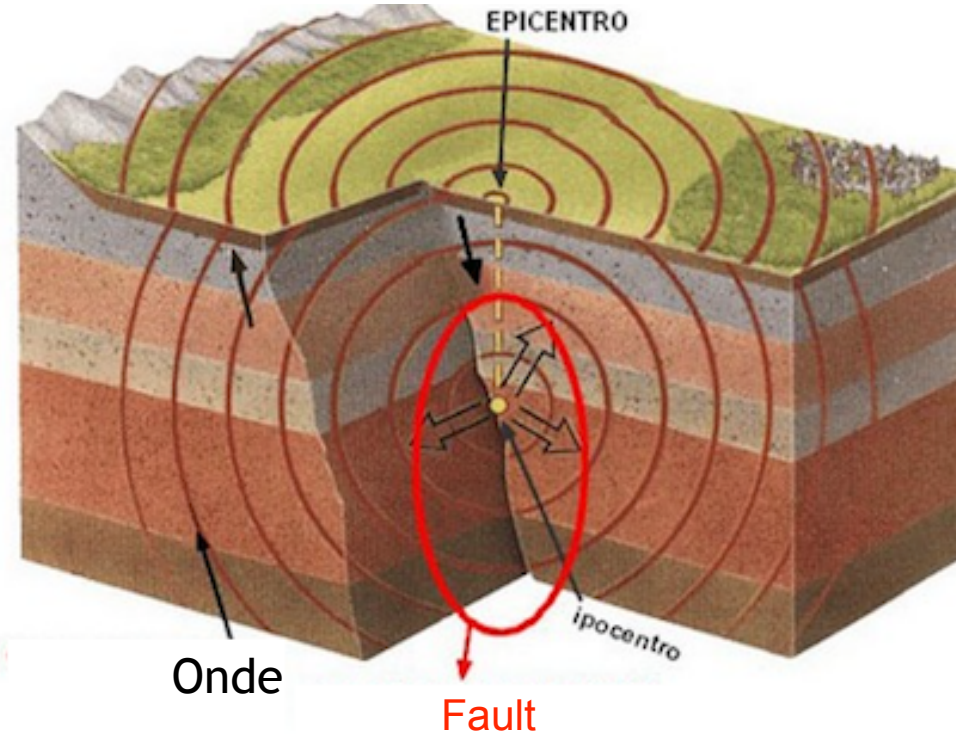


Che cosa genera questo accumulo di energia? Come e perché si attiva una faglia? Capire da dove viene l'energia e che cosa ne caratterizza la dissipazione significa svelare più compiutamente l'origine dei terremoti e forse un giorno poterli prevedere.

# Earthquakes

Pressione e temperatura aumentano scendendo all'interno della Terra, ma hanno l'effetto opposto: la pressione rende le rocce più stabili, mentre la temperatura le rende più deboli.

La conseguenza di questa antitesi fa sì che la crosta terrestre sia divisa in due parti caratterizzate dal diverso comportamento meccanico delle rocce.

Nella crosta superiore, spessa in media 15 chilometri, domina l'effetto della pressione, rendendo le rocce stabili e fragili, mentre nella crosta inferiore, corrispondente ai sottostanti 15 chilometri, prevale l'effetto della temperatura, che rende le rocce deformabili e duttili.

La transizione tra questi due strati a diverso comportamento meccanico, detta anche «transizione fragile-duttile», corrisponde alla massima resistenza delle rocce. Questa è la profondità a cui è necessaria l'energia massima per romperle.

# Earthquakes

L'energia più grande liberata dai terremoti si concentra dunque a circa 15 km di profondità.

Nella crosta inferiore il movimento e la relativa deformazione delle rocce avvengono quasi in regime stazionario, in modo assai lento ma inesorabile, in un ambiente duttile.

Nella crosta superiore fragile, invece, il movimento è episodico: la faglia può rimanere bloccata per anni o per secoli, e rompersi con un forte terremoto, recuperando in pochi secondi buona parte del movimento effettuato dalla parte duttile sottostante nel lungo periodo, detto intersismico, non caratterizzato da forti terremoti.

Il volume fragile sovrastante, rimanendo bloccata la faglia, accumula sforzo, diventando una sorta di batteria energetica.

# Hypocenter, Epicenter

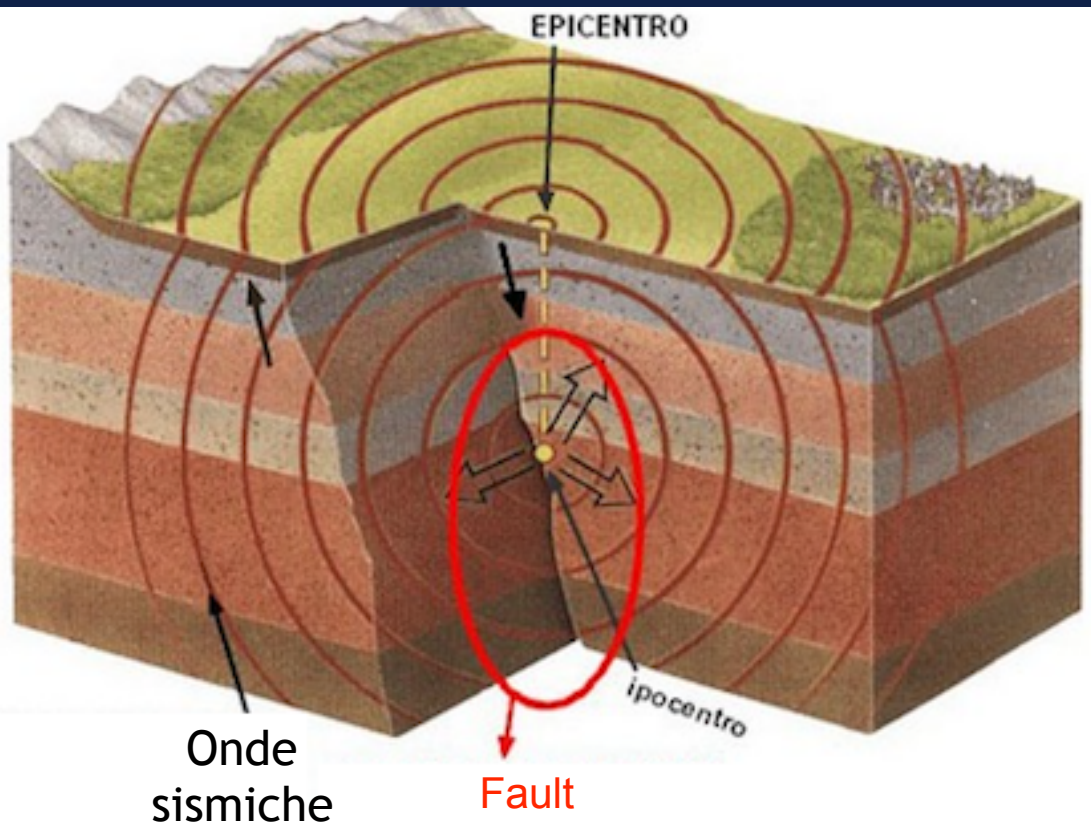


An earthquake is thus the release of energy caused by a sudden slip on a fault (a planar fracture or discontinuity in a volume of rock).

An earthquake's hypocenter is the position where the strain energy stored in the rock is first released, marking the point where the fault begins to rupture.

The fracture generates elastic waves, called seismic waves

Epicenter: the place of the earth's surface located on the vertical hypocenter

# Geodynamics: P and S waves

- There are different kind of seismic waves. The most important ones are
  - Compressional or P (primary)
  - Transverse or S (secondary)
  - Love
  - Rayleigh
- An earthquake radiates P and S waves in all directions.
- The interaction of the P and S waves with Earth's surface $\rightarrow$ surface waves.
- P and S waves travel at different speeds (used to locate earthquakes)

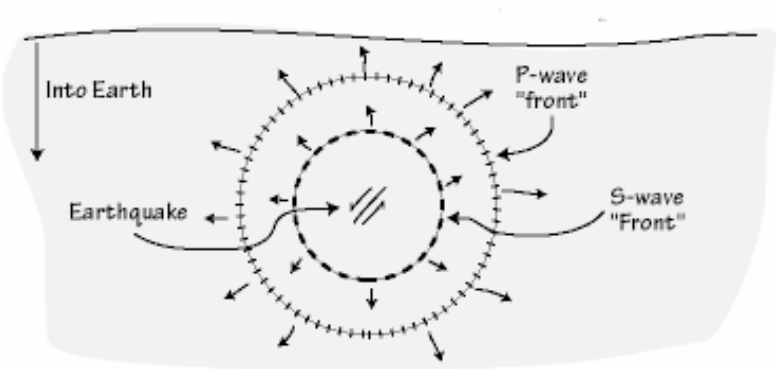


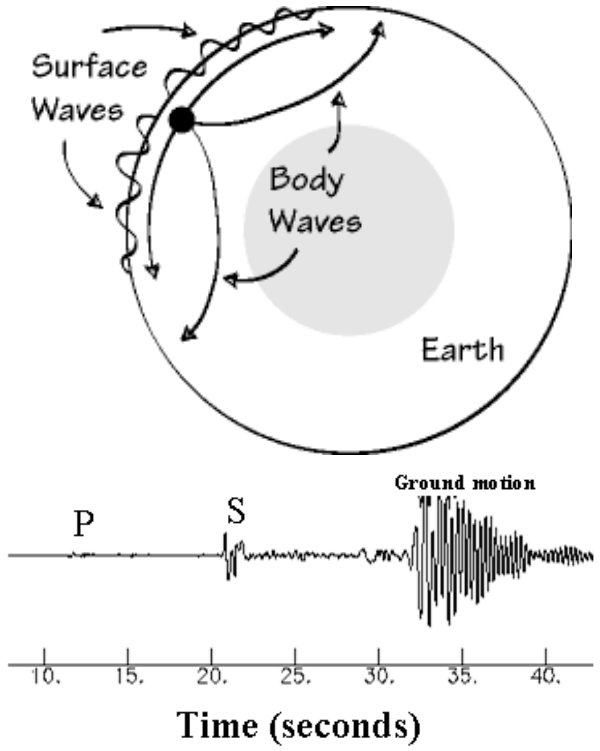

# P and S waves - continues

## P-Waves (Compressional)

- The ground is vibrated in the direction the wave is propagating.
- Travel through all types of media.
- $C_P = \sqrt{(\lambda + 2\mu)/\rho}$ (P-wave velocity)
- Typical speed: $\sim 1 \to 14$ km/sec

## S-Waves (Transverse)

- The ground is vibrated in the perpendicular direction to that the wave is propagating.
- Travel only through solid media.
- $C_S = \sqrt{\mu/\rho}$ (S-wave velocity)
- Typical speed: $\sim 1 \to 8$ km/sec

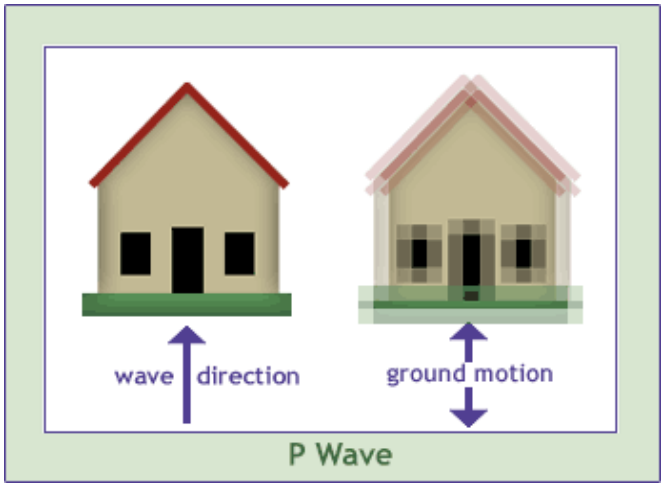


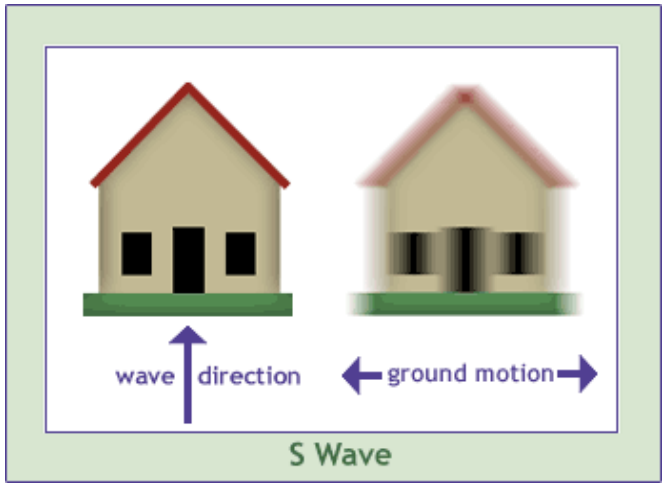


Much of the damage close to an earthquake is the result of strong shaking caused by S-waves.

# Speed of seismic waves in the Earth

Speeds of seismic waves in the Earth

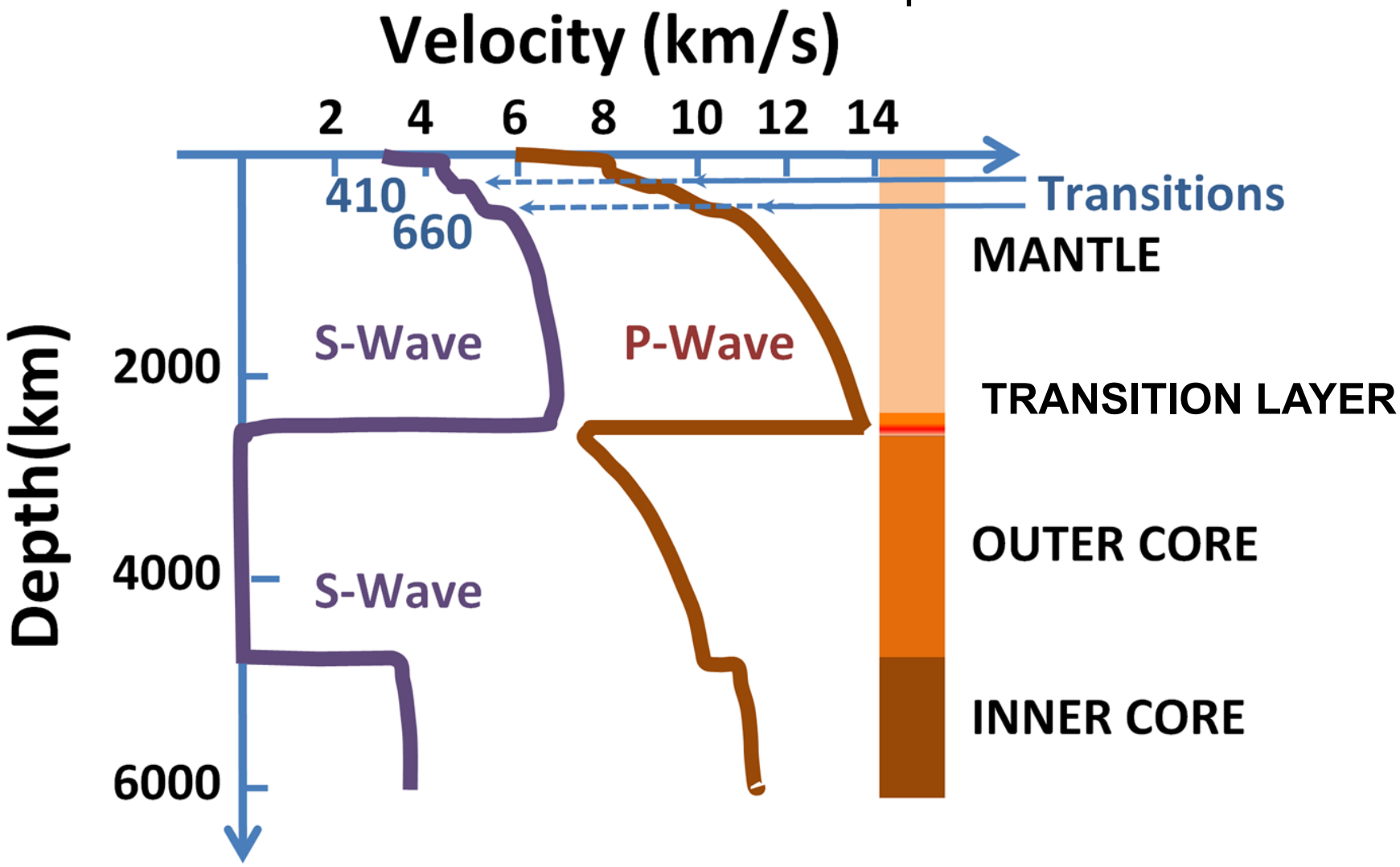


GR Helffrich & BJ Wood (2002). "The Earth's Mantle". Nature. Macmillan Magazines. 412: 501

# Measuring the size of an earthquake

The magnitude is a number that characterises the relative size of an earthquake. Magnitude is based on measurement of the maximum motion recorded by a seismograph.

Magnitudes are based on a logarithmic scale (base 10). Several scales have been defined:

1. Local magnitude - $M_L$
2. Surface-wave magnitude - $M_s$
3. Body-wave magnitude - $M_b$
4. Moment magnitude $M_w$.

Scales 1-3 have limited range and applicability and do not satisfactorily measure the size of the largest earthquakes.

The moment magnitude (Mw) scale, based on the concept of seismic moment, is uniformly applicable to all sizes of earthquakes.

Source USGS

# Moment Magnitude Scale ($M_w$)

$$M_w = (2/3)\log_{10} M_0 - C$$

Seismic moment [N · m].
(~ area of the rupture along the geologic fault where the earthquake occurred × average displacement)

| Magnitudo | TNT equivalente | | Frequenza |
|---|---|---|---|
| 0 | 1,0 | chilogrammo | circa 8.000 al giorno |
| 1 | 31,6 | chilogrammi | |
| 1,5 | 178,0 | chilogrammi | |
| 2 | 1,0 | tonnellata | circa 1.000 al giorno |
| 2,5 | 5,6 | tonnellate | |
| 3 | 31,6 | tonnellate | circa 130 al giorno |
| 3,5 | 178,0 | tonnellate | |
| 4 | 1.000,0 | tonnellate | circa 15 al giorno |
| 4,5 | 5.600,0 | tonnellate | |
| 5 | 31.600,0 | tonnellate | 2-3 al giorno |
| 5,5 | 178.000,0 | tonnellate | |
| 6 | 1,0 | milione di tonnellate | 120 all'anno |
| 6,5 | 5,6 | milioni di tonnellate | |
| 7 | 31,6 | milioni di tonnellate | 18 all'anno |
| 7,5 | 178,0 | milioni di tonnellate | |
| 8 | 1,0 | miliardo di tonnellate | 1 all'anno |
| 8,5 | 5,6 | miliardi di tonnellate | |
| 9 | 31,6 | miliardi di tonnellate | 1 ogni 20 anni |
| 10 | 1.000,0 | miliardi di tonnellate | Mai registrata |

Bomba Hiroshima.
TNT equivalente:
15.000 tonnellate

An increase of one step on the logarithmic scale corresponds to a $10^{1.5} \approx 32$ times increase in the amount of energy released

# Earthquakes: large vs medium (Moment magnitude $M_w$)

Maule, Mw 8.8, 27.02.2010

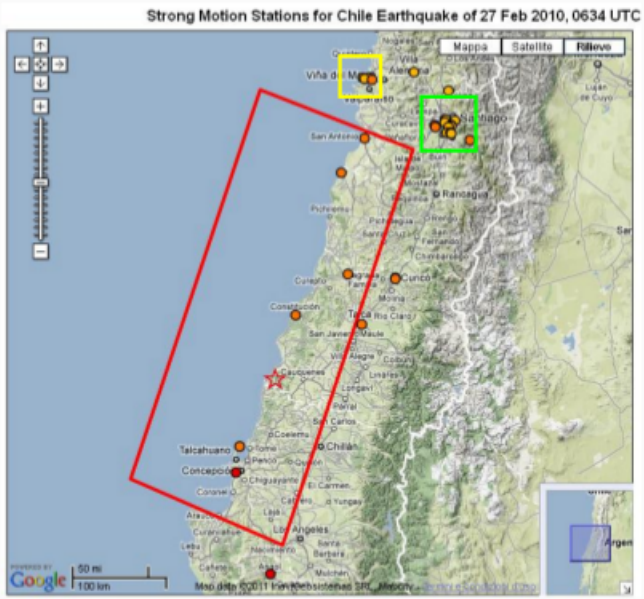


Tohoku, Mw 9.0, 11.03.2011

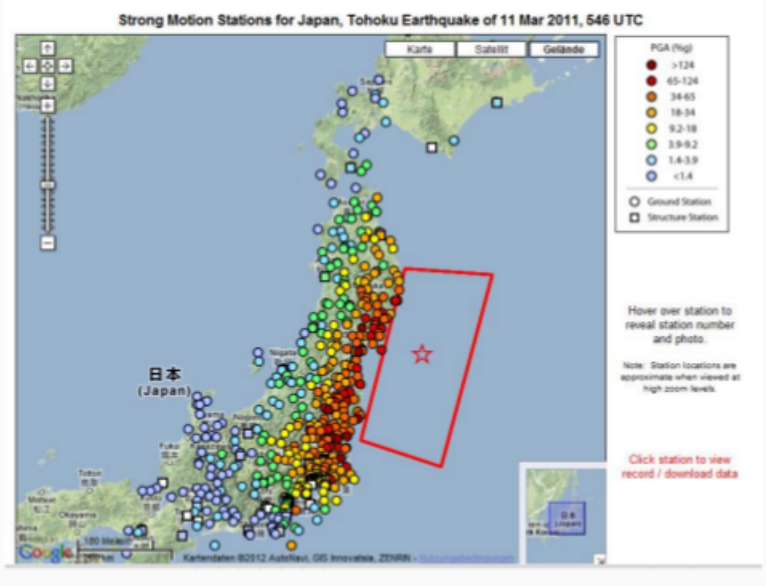


Strong motion stations: Peak Ground Acceleration (PGA)

L'Aquila, Mw 6.1, 06.04.2009

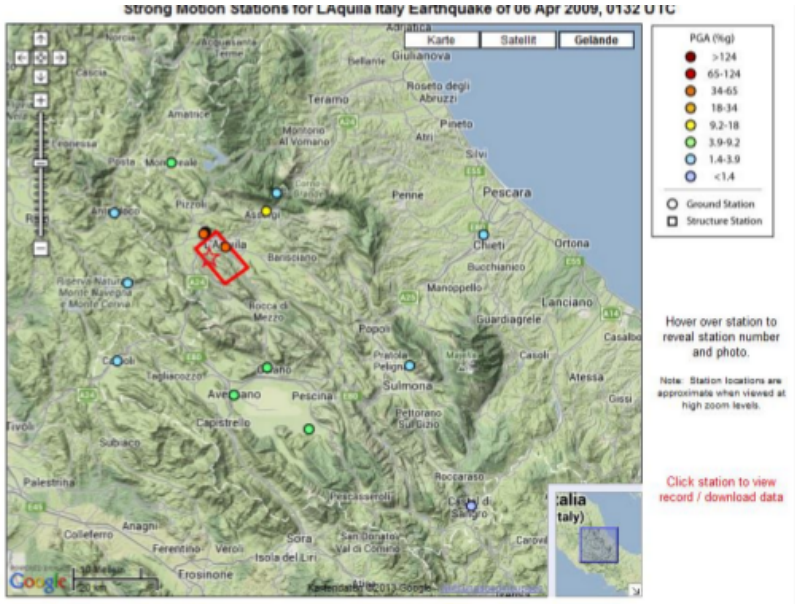


Christchurch Mw 6.3, 22.02.2011

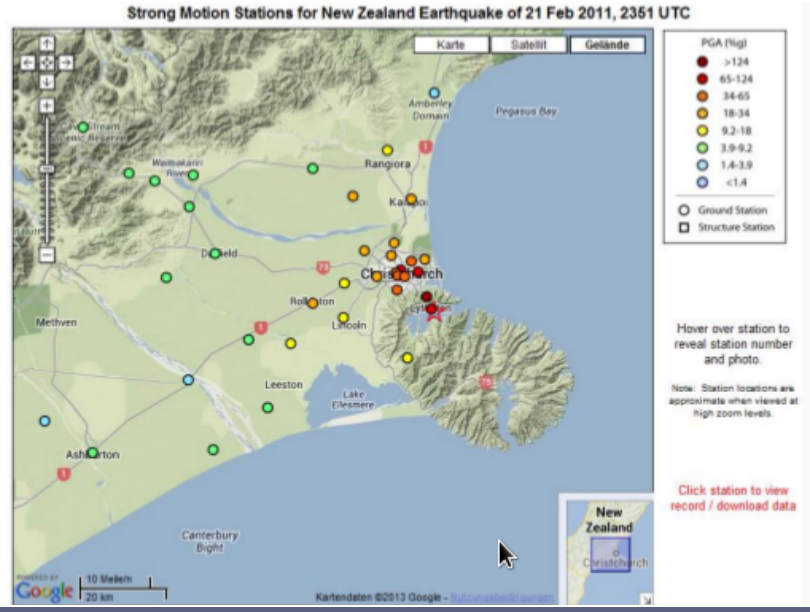

# Italian seismicity: earthquakes since 1900 (Mw≥5.8)

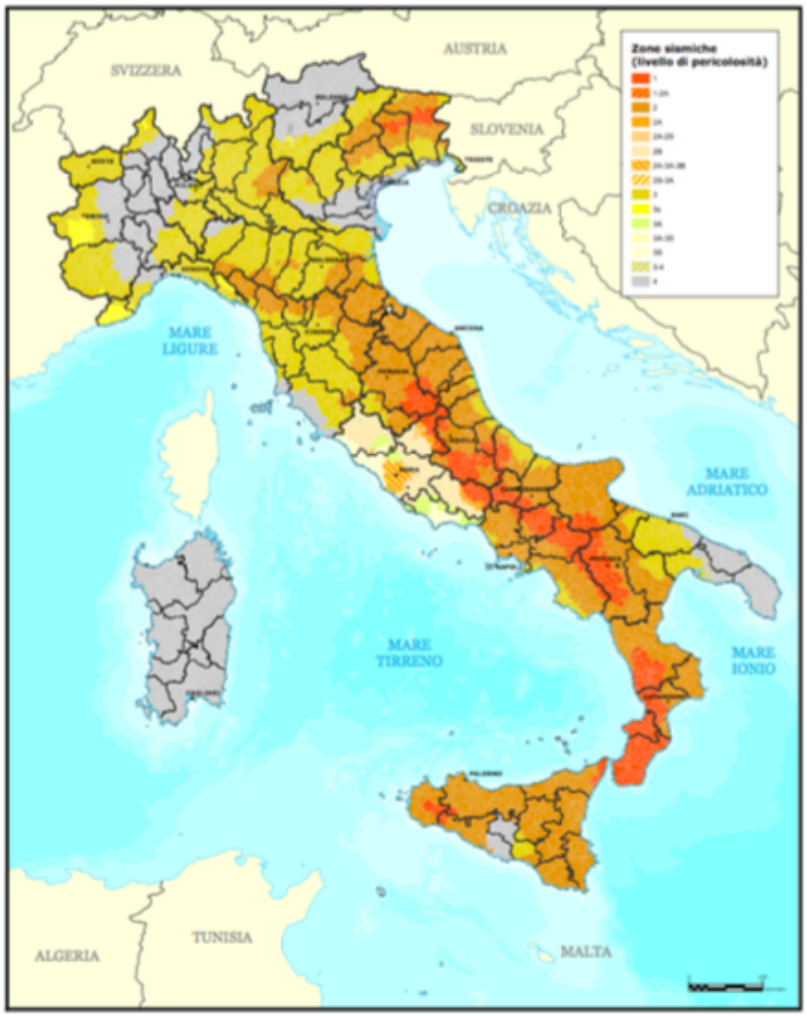


Italian earthquake potential hazard, 2015 (source: Italian Civil Defence)

Mercalli intensity scale

| Data | Area | Intensità | Magnitudo $M_w$ |
|---|---|---|---|
| 08.09.1905 | Calabria | X – XI | 7.1 |
| 23.10.1907 | Calabria | IX | 5.9 |
| 28.12.1908 | Stretto di Messina (Calabria, Sicilia) | XI | 7.2 |
| 07.06.1910 | Irpinia (Basilicata) | IX | 5.9 |
| 27.10.1914 | Garfagnana (Toscana) | VII | 5.8 |
| 13.01.1915 | Avezzano (Abruzzo) | XI | 7.0 |
| 17.05.1916 | Mar Adriatico settentrionale | VIII | 5.9 |
| 16.08.1916 | Mar Adriatico settentrionale | VIII | 5.9 |
| 26.04.1917 | Monterchi – Citerna (Toscana – Umbria) | IX – X | 5.8 |
| 10.11.1918 | Appennino forlivese (Emilia Romagna) | VIII | 5.8 |
| 29.06.1919 | Mugello (Toscana) | IX | 6.2 |
| 07.09.1920 | Garfagnana (Toscana) | X | 6.5 |
| 07.03.1928 | Capo Vaticano (Calabria) | VIII | 5.9 |
| 23.07.1930 | Irpinia (Campania) | X | 6.7 |
| 30.10.1930 | Senigallia (Marche) | VIII – IX | 5.9 |
| 18.10.1936 | Bosco Cansiglio (Veneto) | IX | 5.9 |
| 03.10.1943 | Ascolano (Marche) | IX | 5.8 |
| 21.08.1962 | Irpinia (Campania) | IX | 6.2 |
| 15.01.1968 | Valle del Belice (Sicilia) | X | 6.1 |
| 06.05.1976 | Friuli | IX – X | 6.4 |
| 15.09.1976 | Friuli | VIII – IX | 5.9 |
| 15.04.1978 | Golfo di Patti (Sicilia) | VIII | 6.1 |
| 19.09.1979 | Valnerina (Umbria) | VIII – IX | 5.9 |
| 23.11.1980 | Irpinia (Campania, Basilicata) | X | 6.9 |
| 07.05.1984 | Lazio – Abruzzo | VIII | 5.9 |
| 05.05.1990 | Potentino (Basilicata) | VII – VIII | 5.8 |
| 26.09.1997 | Umbria – Marche | IX | 6.0 |
| 31.10.2002 | Molise | VIII – IX | 5.8 |
| 06.04.2009 | Abruzzo | IX – X | 6.1# |
| 20.05.2012 | Pianura Padana Emiliana (Emilia Romagna) | VIII* | 5.8# |
| 29.05.2012 | | | 5.6# |

# Dati: iside.rm.ingv.it
* Cumulo degli effetti della sequenza

(Source: CPTI11, http://emidius.mi.ingv.it/CPTI11/).

# Ground motion prediction (GMP)

Tools for ground motion prediction (GMP) are one of the key ingredients in seismic hazard analysis, both within probabilistic and deterministic frameworks.

Objective: provide estimates of the expected ground motion at a site, given an earthquake of known magnitude, distance, faulting style, etc.

A variety of procedures for GMP relying on different information detail on the seismic source and propagation path on one side, and, on the other side, providing different levels of output, either in terms of peak values of ground motion or of an entire time history.

Proposed procedures range from the empirical Ground Motion Prediction Equations (GMPE), typically calibrated on the instrumental observations from real earthquakes, up to complex 3D Physics-Based numerical Simulations (PBS).

# Approaches for ground motion prediction

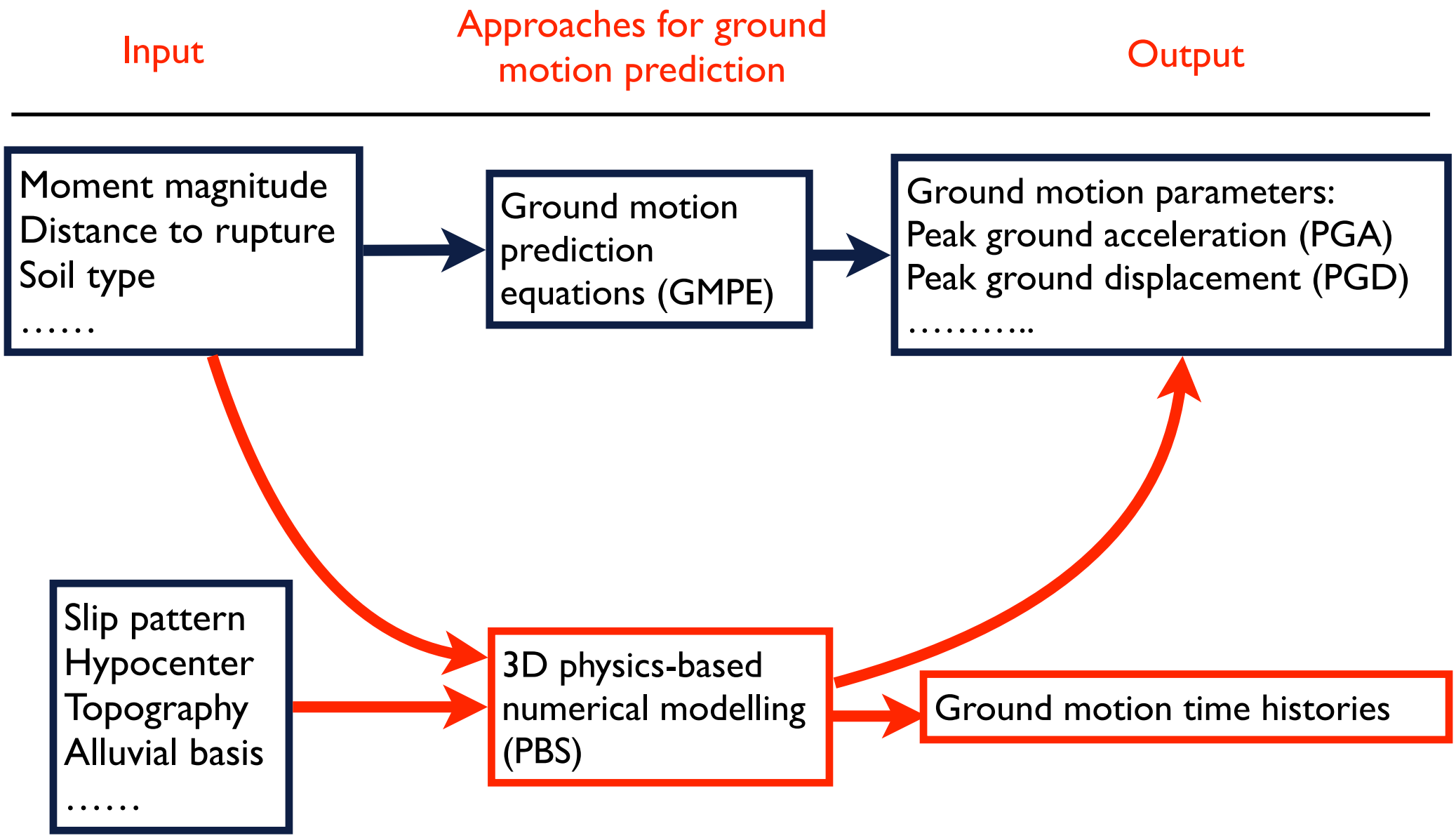

# Seismic risk in nutshell

Hazard: probability that an earthquake will occur in a given geographic area within a given window of time, and with ground motion intensity exceeding a given threshold

Vulnerability: inability of buildings to withstand the effects of seismic forces

Exposure: possibility of damage in economic terms, to cultural heritage or the loss of human lives

Assess the vulnerability of existing buildings is an essential step to improve seismic risk management

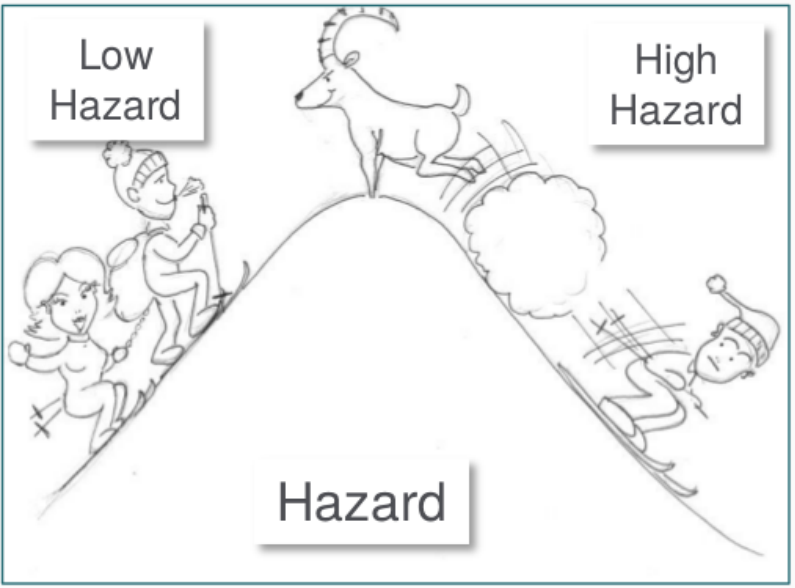



# From ground motion prediction to seismic vulnerability of structures

Numerical modeling

Ground motion time histories/parameters

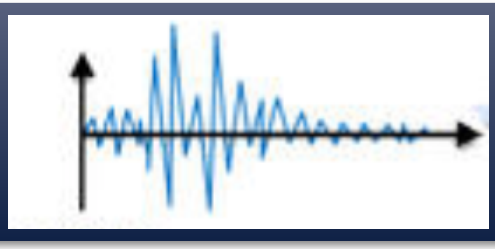

Fragility curves: conditional probability of failure at a given seismic response parameter (PGA, PGV, …..)

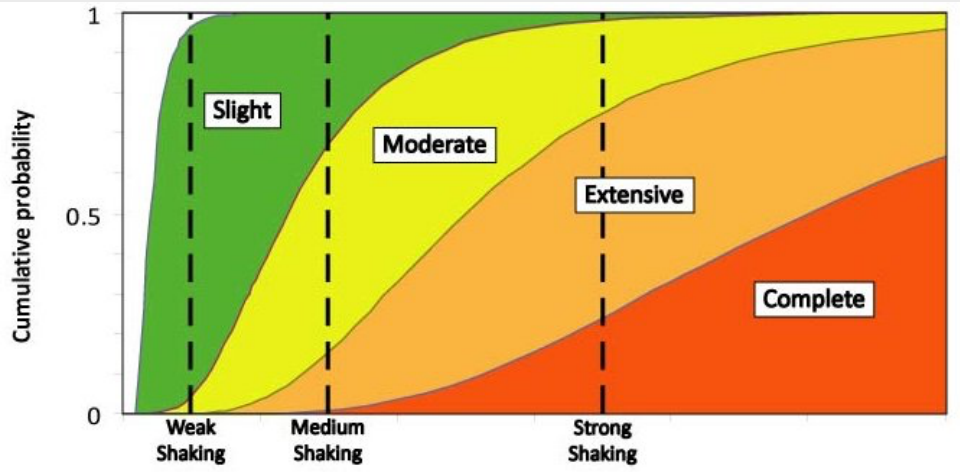


Structural analysis based on mathematical/numerical modelling of the building

# Limitations of Ground Motion Prediction Equations

The amount of available earthquake records

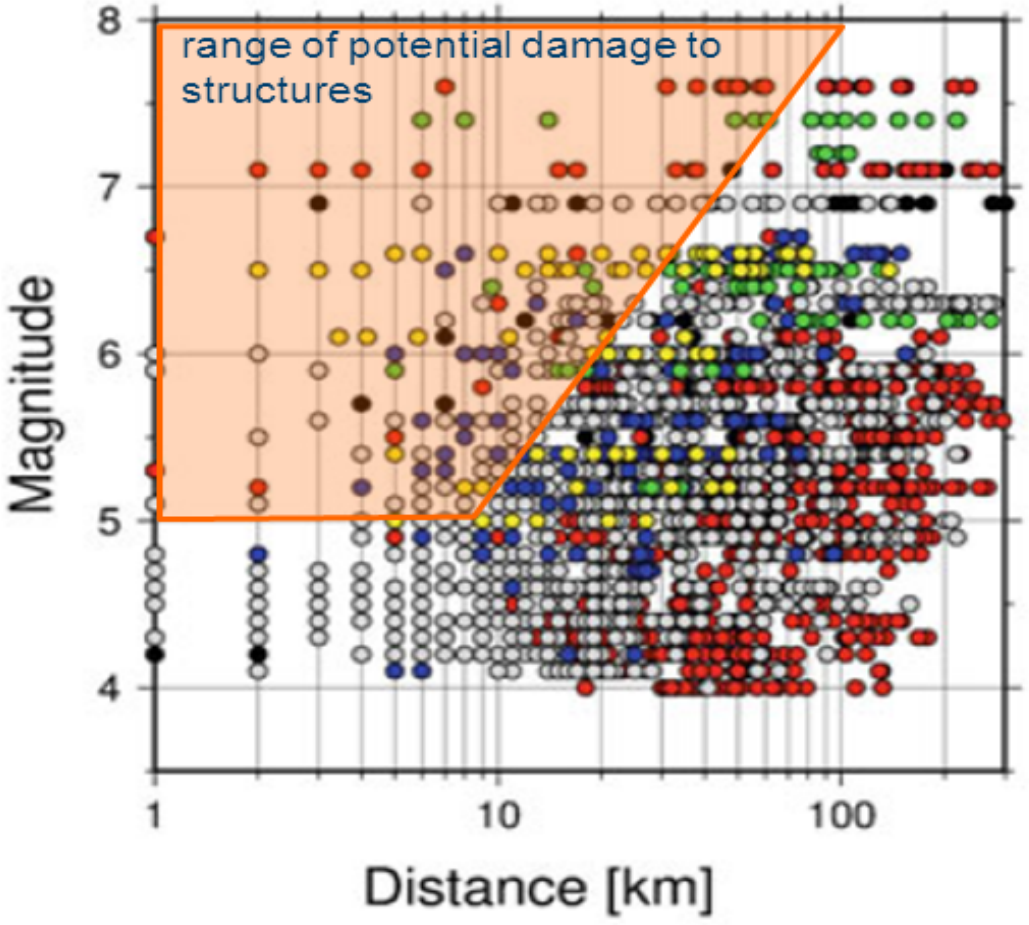


Turkey

Italy

Greece

Iran

Iceland

Other countries

Magnitude and distance range covered by the strong motion database for calibration of pan-European ground motion prediction equations

# PBS - The mathematical model

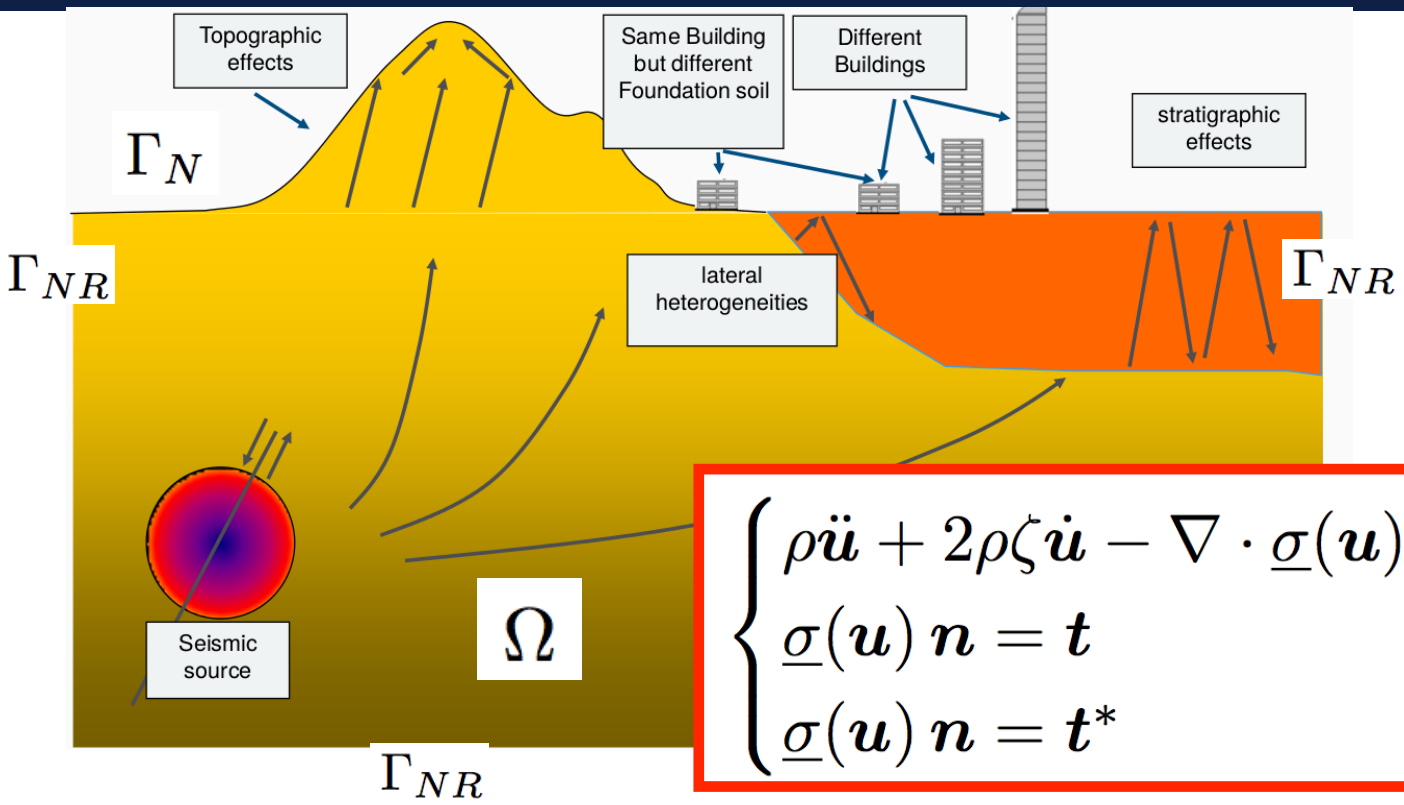


$$\begin{cases} \rho\ddot{\boldsymbol{u}} + 2\rho\zeta\dot{\boldsymbol{u}} - \nabla\cdot\underline{\sigma}(\boldsymbol{u}) + \rho\zeta^2\boldsymbol{u} = \boldsymbol{f} & \text{in } \Omega \\ \underline{\sigma}(\boldsymbol{u})\,\boldsymbol{n} = \boldsymbol{t} & \text{on } \Gamma_N \\ \underline{\sigma}(\boldsymbol{u})\,\boldsymbol{n} = \boldsymbol{t}^* & \text{on } \Gamma_{NR} \end{cases}$$

$\boldsymbol{u} = \boldsymbol{u}(\boldsymbol{x}, t)$ is the displacement field

$\underline{\sigma}(\boldsymbol{u}) = \lambda \mathrm{tr}(\underline{\epsilon}(\boldsymbol{u}))\underline{I} + 2\mu\underline{\epsilon}(\boldsymbol{u})$ is the stress tensor

$\zeta \geq 0$ is a dumping factor (~0.01 $s^{-1}$)

$\lambda = \lambda(\boldsymbol{x})$ $\mu = \mu(\boldsymbol{x})$ are the first/second Lame' coefficients

The term $2\rho\zeta\dot{\boldsymbol{u}} + \rho\zeta^2\boldsymbol{u}$ models the visco-elastic effects

$\rho$ is the medium density

$\boldsymbol{t}^* = \boldsymbol{t}^*(\boldsymbol{x}, t)$ is a fictitious traction

$\boldsymbol{t} = \boldsymbol{t}(\boldsymbol{x}, t)$ is a given traction

$$c_P = \sqrt{\frac{\lambda + 2\mu}{\rho}}, \qquad c_S = \sqrt{\frac{\mu}{\rho}},$$

compressional/shear wave velocities

# Weak form

$\forall t \in (0,T]$ find $\boldsymbol{u}(t) \in \boldsymbol{V} = \{\boldsymbol{v} \in \boldsymbol{H}^1(\Omega),\ \boldsymbol{v} = \boldsymbol{0} \text{ on } \Gamma_D\}$ such that

$$(\rho\ddot{\boldsymbol{u}}(t), \boldsymbol{v})_\Omega + (2\rho\zeta\dot{\boldsymbol{u}}(t), \boldsymbol{v})_\Omega + (\rho\zeta^2\boldsymbol{u}, \boldsymbol{v})_\Omega + \mathcal{A}(\boldsymbol{u}(t), \boldsymbol{v}) = \mathcal{F}(\boldsymbol{v}) \qquad \forall \boldsymbol{v} \in V$$

supplemented with the initial conditions $\boldsymbol{u}(0) = \boldsymbol{u}_0$ and $\dot{\boldsymbol{u}}(0) = \boldsymbol{v}_0$

$$\mathcal{A}(\boldsymbol{u}, \boldsymbol{v}) = (\underline{\sigma}(\boldsymbol{u}), \underline{\varepsilon}(\boldsymbol{v}))_\Omega, \quad \mathcal{F}(\boldsymbol{v}) = (\boldsymbol{f}, \boldsymbol{v})_\Omega + \langle \boldsymbol{t}, \boldsymbol{v} \rangle_{\Gamma_N} + \langle \boldsymbol{t}^*, \boldsymbol{v} \rangle_{\Gamma_{NR}}.$$

# Requirements on the numerical solution

- Accurate description of the behaviour at material interfaces
  - ⇨ high-order accuracy
- Waves are typically propagated over many periods of time
  - ⇨ control the numerical dispersion and dissipation errors
- Complex geometries and strong contrasts in wave speeds
  - ⇨ methods that accommodate non-conforming grids
- The size of the bodies excited is large relative to the wavelengths of interests
  - ⇨ efficient and scalable implementation for parallel computing

**Discontinuous Galerkin Spectral Element methods (DGSEM)**

Discontinuous Galerkin methods for wave propagation problems

[Riviere, Wheeler, 2003], [Riviere, Shaw, Wheeler, Whiteman, 2003],[Kaser, Dumbser, 2006], [Chung, Enquist, 2006], [Riviere, Shaw, Whiteman, 2007], [De Basabe, Sen, 2007], [Dumbser, Kaser, Toro, 2007], [de Basabe, Sen, Wheeler, 2008], [Delcourte, Fezoui, Glinsky-Olivier, 2009],[Grote, Diaz, 2009], [Wilcox, Stadler, Burstedde, Ghattas, 2010], [Etienne, Chaljub,Virieux, Glinsky, 2010], [Antonietti, Mazzieri, Rapetti, Quarteroni, 2012], [Pelties, Puente, Ampuero, Brietzke, Kaser. 2012], [Mazzieri, Stupazzini, Smerzini, Guidotti, 2013], [Peyrusse, Glinsky, Gelis, Lanteri, 2014], [Antonietti, Ayuso, Mazzieri, Quarteroni, 2015], [Antonietti, Marcati, Mazzieri, Quarteroni, 2015], [Paolucci, Mazzieri, Smerzini, 2015], [Mercerat, Glinsky, 2015], [Antonietti, Dal Santo, Mazzieri, Quarteroni, 2016], [Ferroni, Antonietti Mazzieri, Quarteroni, 2016], [Antonietti, Ferroni, Mazzieri, Paolucci, Quarteroni, Smerzini, Stupazzini, 2017]

# Mesh partition and subspaces

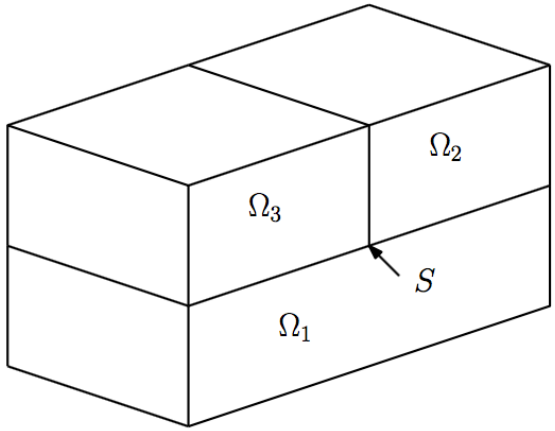


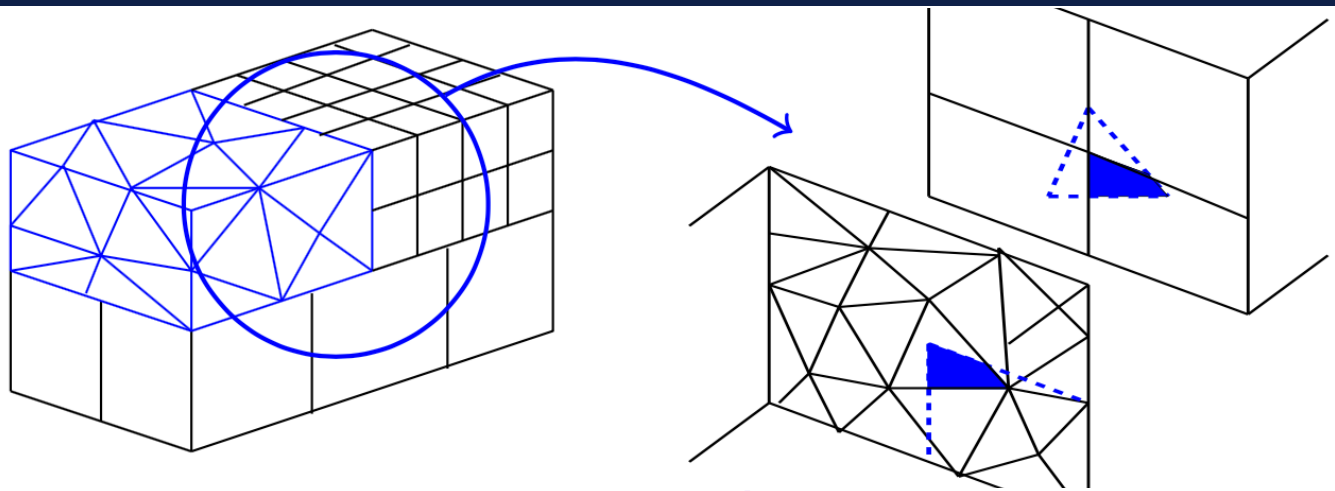

$\Omega$ is partitioned into macro-regions $\Omega_i$

Each macro-region is meshed indepen
by a conforming hexahedral/tetrahedra
partition $\mathcal{T}_{h\ell}$

DG paradigm at the interfaces

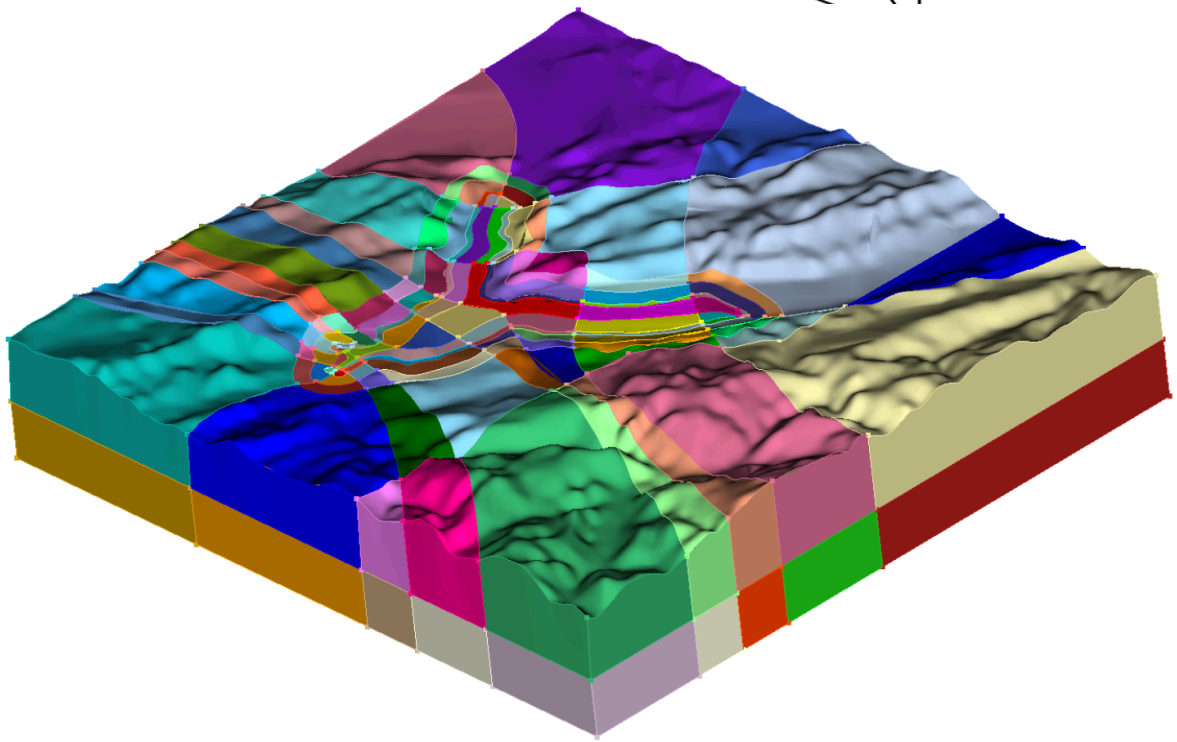

A function in $\boldsymbol{V}_{\mathrm{DG}}$ is

continuous in each macro-region

discontinuous across the skeleton

a polynomial of degree $N_\ell$ in each mesh-element of $\mathcal{T}_{h\ell}$

# The semidiscrete scheme

$$\forall t \in (0,T], \text{ find } \boldsymbol{u}_h = \boldsymbol{u}_h(t) \in \boldsymbol{V}_{\mathrm{DG}} \text{ such that}$$

$$\sum_{\Omega_\ell} (\rho \ddot{\boldsymbol{u}}_h(t), \boldsymbol{v})_{\Omega_\ell} + \sum_{\Omega_\ell} (2\rho\zeta \dot{\boldsymbol{u}}_h(t), \boldsymbol{v})_{\Omega_\ell} + \mathcal{A}_h(\boldsymbol{u}_h(t), \boldsymbol{v}) + \sum_{\Omega_\ell} (\rho\zeta^2 \boldsymbol{u}_h, \boldsymbol{v})_{\Omega_\ell} = \mathcal{F}_h(\boldsymbol{v})$$

$$\mathcal{A}_h(\boldsymbol{u}, \boldsymbol{v}) = \sum_{\Omega_\ell} (\underline{\sigma}(\boldsymbol{u}), \underline{\varepsilon}(\boldsymbol{v}))_{\Omega_\ell} - \langle \{\underline{\sigma}(\boldsymbol{u})\}, [\![\boldsymbol{v}]\!] \rangle_{\mathcal{F}_h^I} - \langle [\![\boldsymbol{u}]\!], \{\underline{\sigma}(\boldsymbol{v})\} \rangle_{\mathcal{F}_h^I} + \langle \eta [\![\boldsymbol{u}]\!], [\![\boldsymbol{v}]\!] \rangle_{\mathcal{F}_h^I},$$

$$\mathcal{F}_h(\boldsymbol{v}) = \sum_{\Omega_\ell} (\mathbf{f}, \boldsymbol{v})_{\Omega_\ell} + \langle \boldsymbol{t}, \boldsymbol{v} \rangle_{\mathcal{F}_h^N} + \langle \boldsymbol{t}^*, \boldsymbol{v} \rangle_{\mathcal{F}_h^{NR}}$$

## Stability

Assume $\boldsymbol{t = 0}$ and $\Gamma_{NR} = \emptyset$

**Theorem** (Stability). *Let, for any time $t \in (0,T]$ and for a sufficiently large penalty parameter $\boldsymbol{u}_h(t) \in \boldsymbol{V}_{\mathrm{DG}}$ be the semi-discrete solution. If $\boldsymbol{f} \in L^2(0,T;\boldsymbol{L}^2(\Omega))$, then*

$$\|\boldsymbol{u}_h(t)\|_{\mathcal{E}} \lesssim \|\boldsymbol{u}_h(0)\|_{\mathcal{E}} + \int_0^t \|\boldsymbol{f}(\tau)\|_{0,\Omega}\, d\tau, \quad 0 < t \leq T.$$

$$\|\boldsymbol{u}_h(t)\|_{\mathcal{E}}^2 = \|\rho^{1/2}\dot{\boldsymbol{u}}_h(t)\|_{0,\Omega}^2 + \|\rho^{1/2}\zeta \boldsymbol{u}_h(t)\|_{0,\Omega}^2 + \sum_\ell \|\underline{D}^{1/2}\underline{\varepsilon}(\boldsymbol{v})\|_{0,\Omega_\ell}^2 + \|\eta^{1/2}[\![\boldsymbol{v}]\!]\|_{0,\mathcal{F}_h^I}^2$$

# Error estimates for the semidiscrete formulation

**Theorem** *(A-priori error estimate in the energy norm.) If* $\boldsymbol{u}(t)|_{\Omega_\ell}, \dot{\boldsymbol{u}}(t)|_{\Omega_\ell}, \ddot{\boldsymbol{u}}(t)|_{\Omega_\ell} \in \boldsymbol{H}^{s_\ell}(\Omega_\ell)$, $\ell = 1, \ldots, L$, $s_\ell \geq 2$, *then*

$$\sup_{t\in[0,t]} \|\boldsymbol{e}_h\|^2_{\mathcal{E}} \lesssim \sup_{t\in[0,T]} \left\{ \sum_{\Omega_\ell} \frac{h_\ell^{2\min(s_\ell, N_\ell+1)-2}}{N_\ell^{2s_\ell-3}} \left( \|\dot{\boldsymbol{u}}\|^2_{s_\ell,\Omega_\ell} + \|\boldsymbol{u}\|^2_{s_\ell,\Omega_\ell} \right) \right\}$$
$$+ \int_0^T \sum_{\Omega_\ell} \frac{h_\ell^{2\min(s_\ell, N_\ell+1)-2}}{N_\ell^{2s_\ell-3}} \left( \|\ddot{\boldsymbol{u}}\|^2_{s_\ell,\Omega_\ell} + \|\dot{\boldsymbol{u}}\|^2_{s_\ell,\Omega_\ell} \right) d\tau.$$

**Remark** *If* $h = \max_{\Omega_\ell} h_\ell \approx h_\ell$, $N_\ell = N$ *for any* $\ell = 1, \ldots, L$, *and the exact solution belong to* $\boldsymbol{H}^s(\Omega)$, *with* $s \geq N+1$,

$$\sup_{t\in[0,T]} \|\boldsymbol{e}_h(t)\|^2_{\mathcal{E}} \lesssim \frac{h^{2\min(s,N+1)-2}}{N^{2s-3}} \left( \sup_{t\in[0,T]} \left\{ \|\dot{\boldsymbol{u}}\|^2_{s,\Omega} + \|\boldsymbol{u}\|^2_{s,\Omega} \right\} + \int_0^T \left( \|\ddot{\boldsymbol{u}}\|^2_{s,\Omega} + \|\dot{\boldsymbol{u}}\|^2_{s,\Omega} \right) d\tau \right)$$

# Fully discrete formulation

The semi-discrete algebraic formulation reads as

$$\begin{aligned} \mathsf{M}\ddot{\mathsf{U}}(t) + (\mathsf{M}_2 + \mathsf{S})\dot{\mathsf{U}}(t) + (\mathsf{A} + \mathsf{M}_3 + \mathsf{R})\mathsf{U}(t) &= \mathsf{F}(t) \\ \mathsf{U}(0) &= \mathsf{U}^0 \\ \dot{\mathsf{U}}(0) &= \mathsf{V}^0 \end{aligned}$$

Second order accurate
Conditionally stabile (CFL)

$$\Delta t \leq C_{CFL} \frac{h}{c_P N^2}$$

Leap-frog time integration scheme

$$\mathsf{M}\mathsf{U}^1 = (\mathsf{M} - \frac{\Delta t^2}{2}\mathsf{Q})\mathsf{U}^0 + (\Delta t \mathsf{M} - \frac{\Delta t^2}{2}\mathsf{K})\mathsf{V}^0 + \frac{\Delta t^2}{2}\mathsf{F}^0,$$

$$(\mathsf{M} + \frac{\Delta t}{2}\mathsf{K})\mathsf{U}^{n+1} = (2\mathsf{M} - \Delta t^2 \mathsf{Q})\mathsf{U}^n + (\mathsf{M} - \frac{\Delta t}{2}\mathsf{K})\mathsf{U}^{n-1} + \Delta t^2 \mathsf{F}^n, \quad n = 1, ..., N_T - 1$$

with $\mathsf{K} = \mathsf{M}_2 + \mathsf{S}$ and $\mathsf{Q} = \mathsf{A} + \mathsf{M}_3 + \mathsf{R}$

# PBS Math is non-destructive

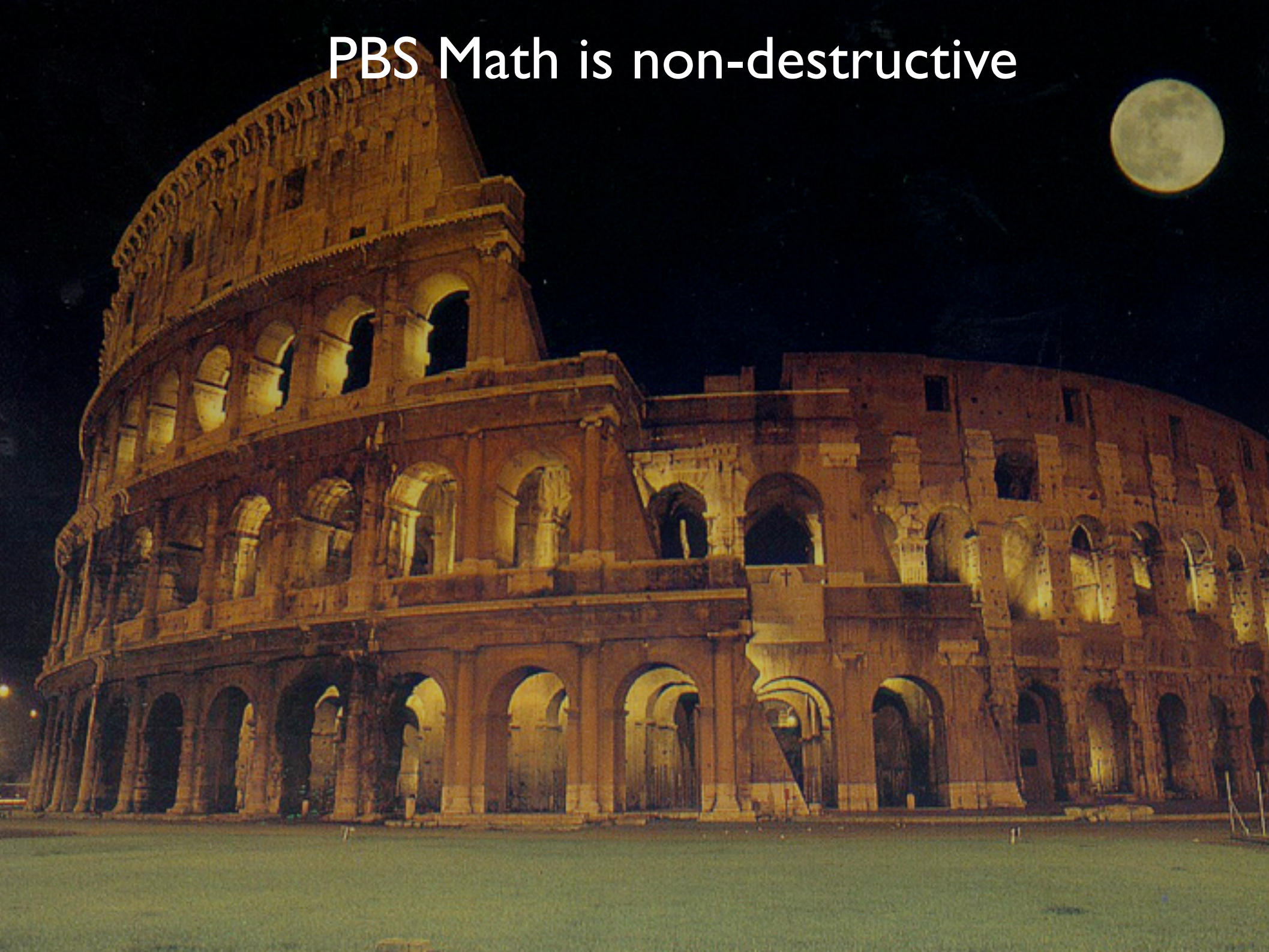

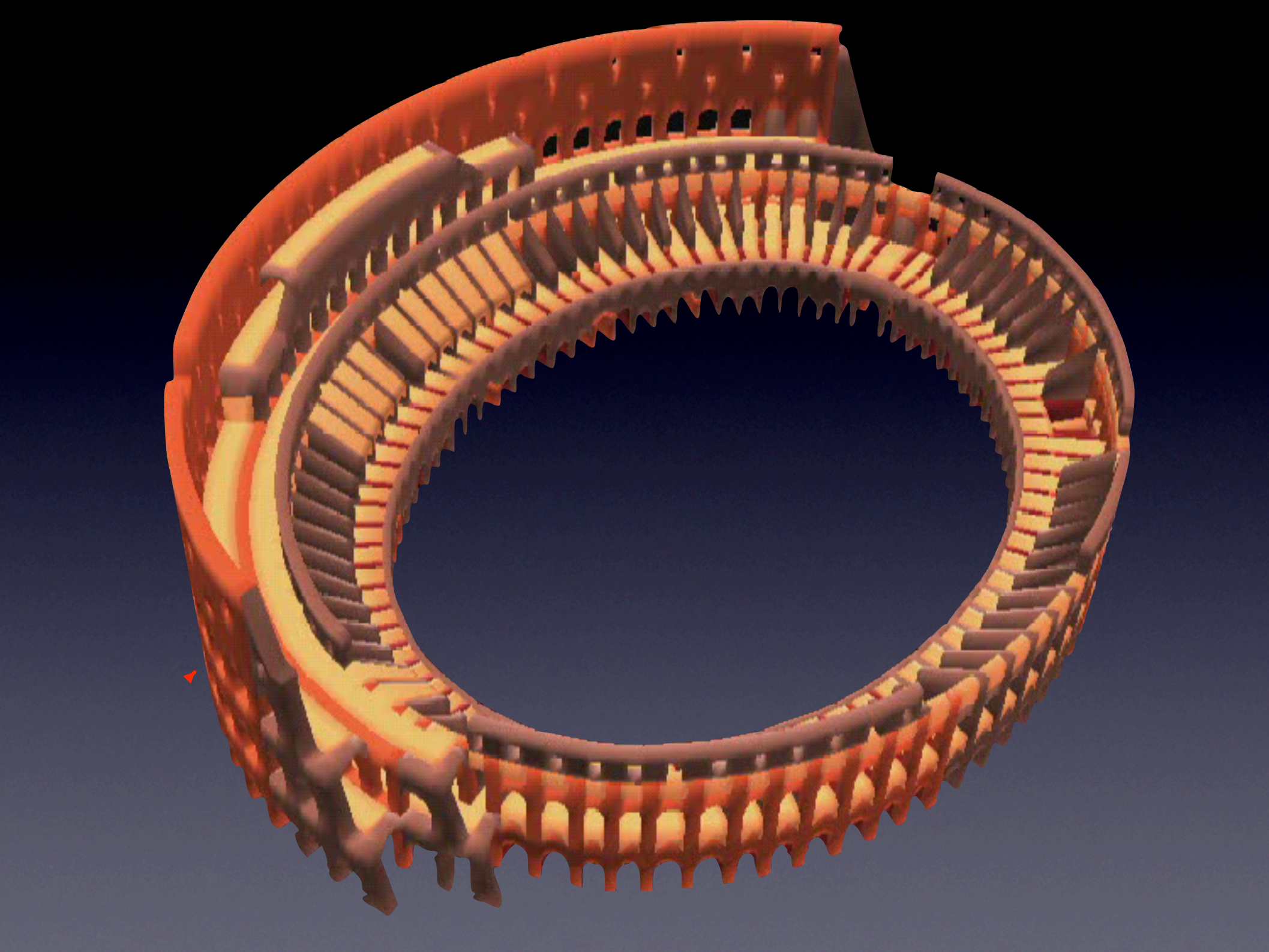

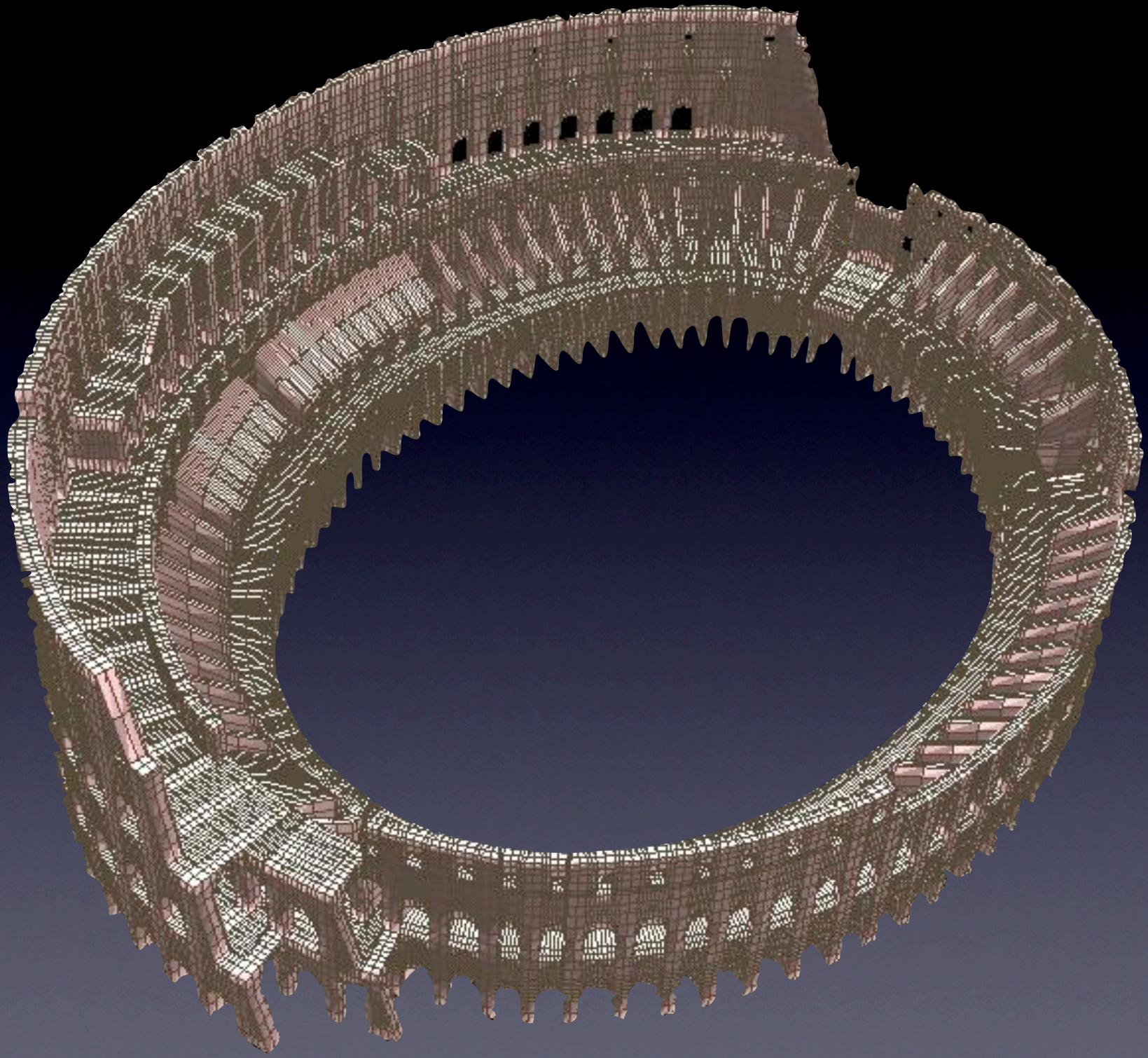

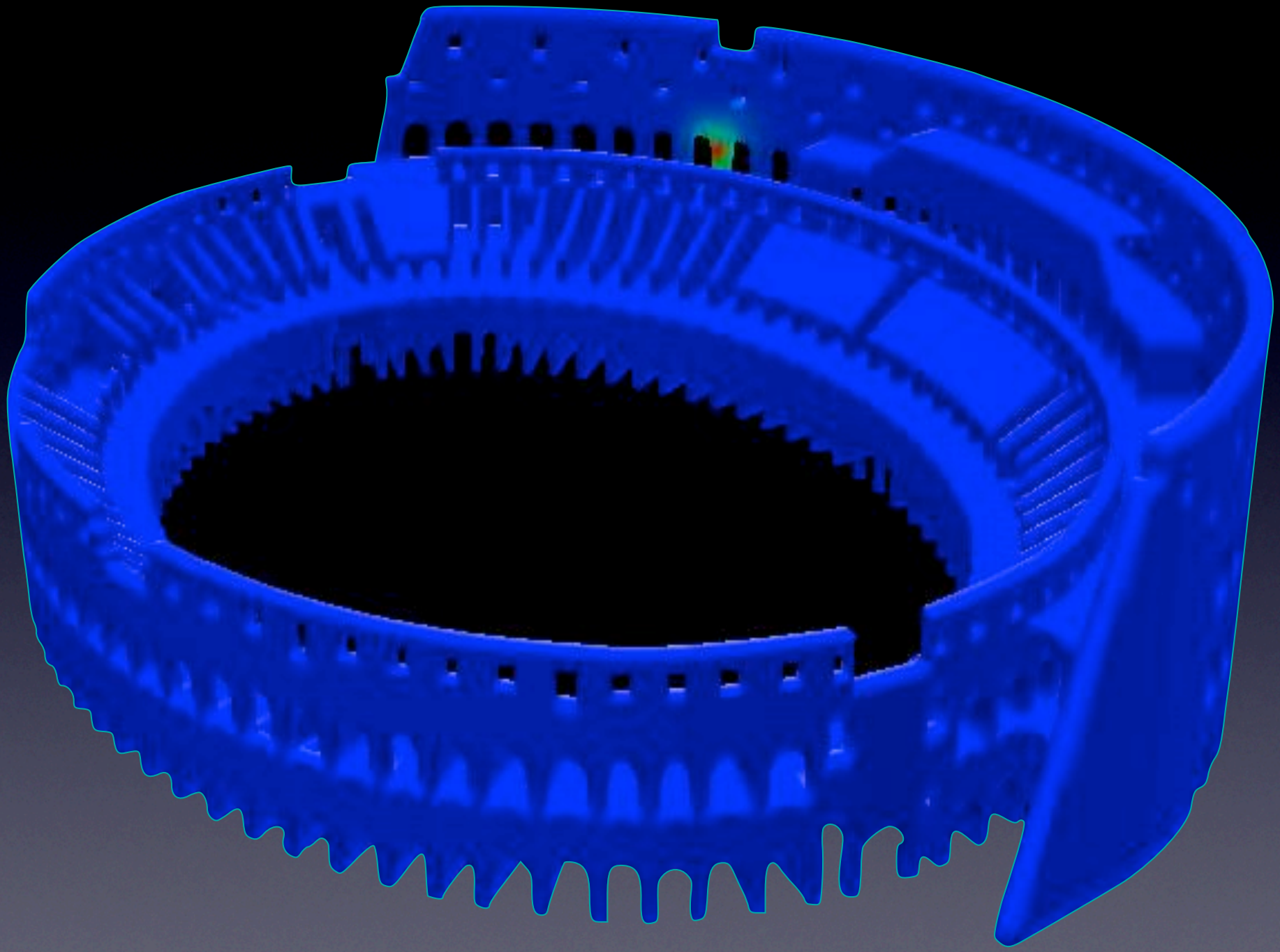

Maggio-Massidda-Fotia @ CRS4

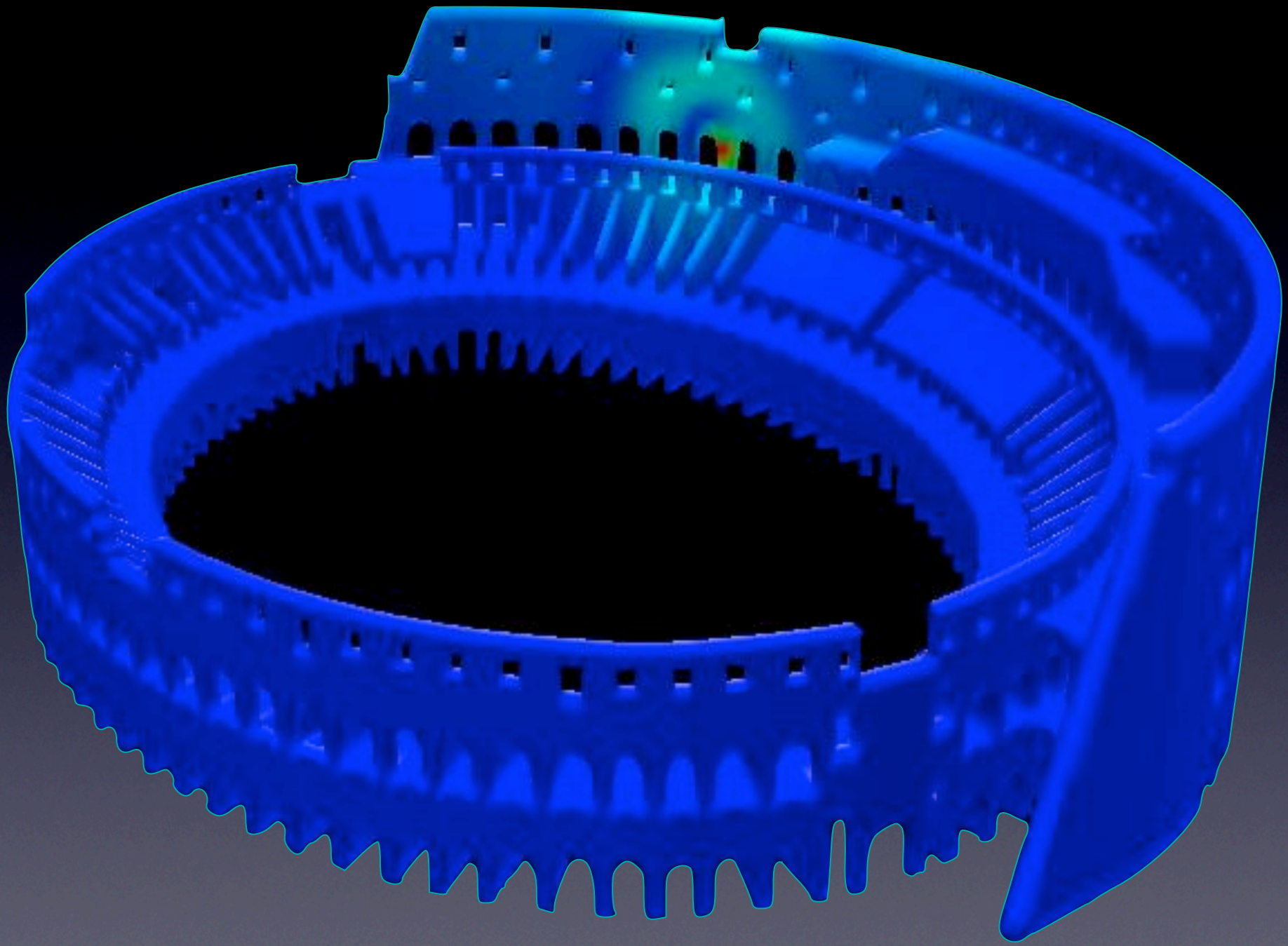

Maggio-Massidda-Fotia @ CRS4

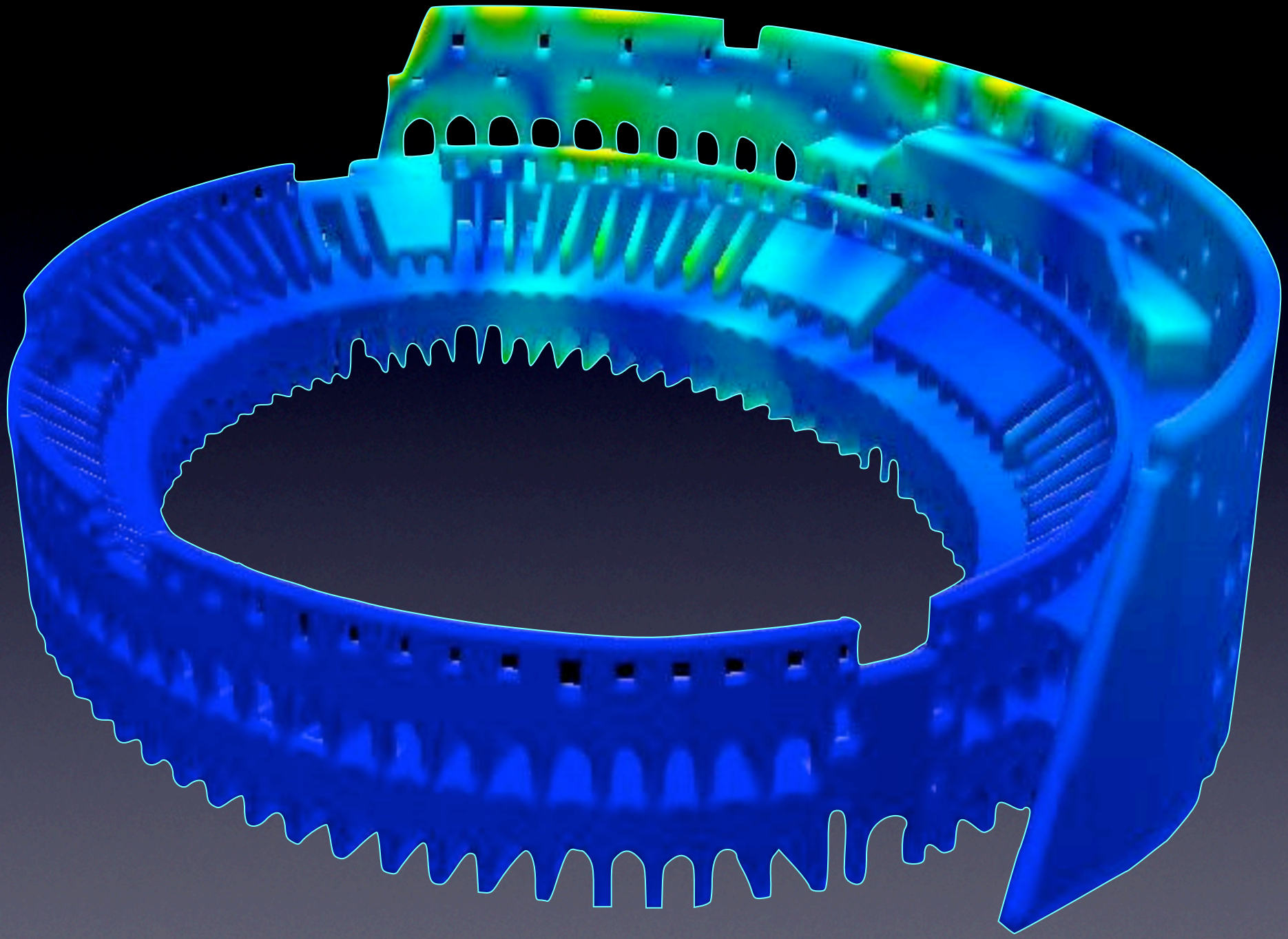

Maggio-Massidda-Fotia @ CRS4


# Geodynamics
# Earthquakes impact on civil structures
# Acquasanta Railway bridge, Liguria, Italy

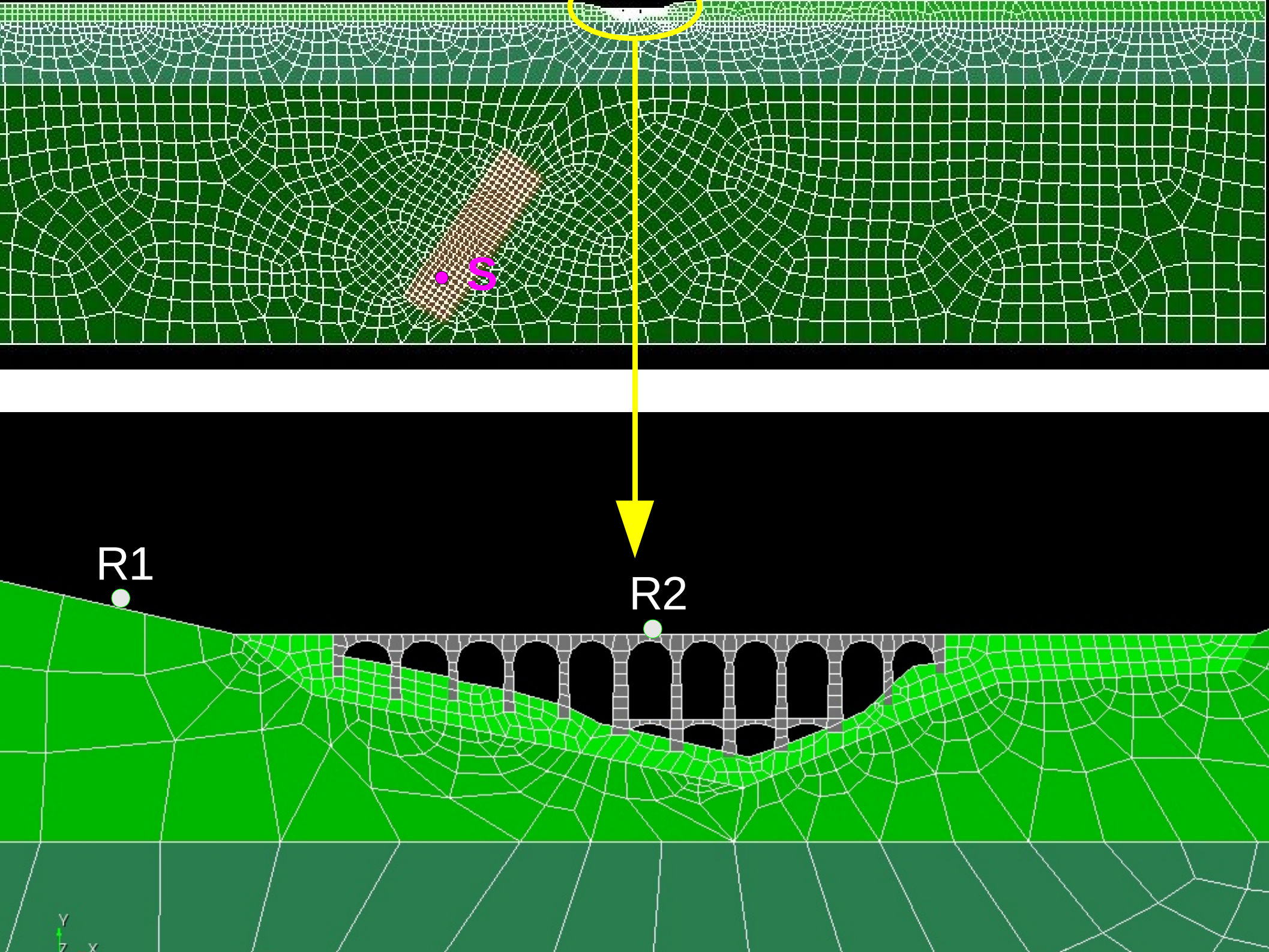
S
R1
R2
Y
Z
X

# Acquasanta Railway bridge, Liguria, Italy

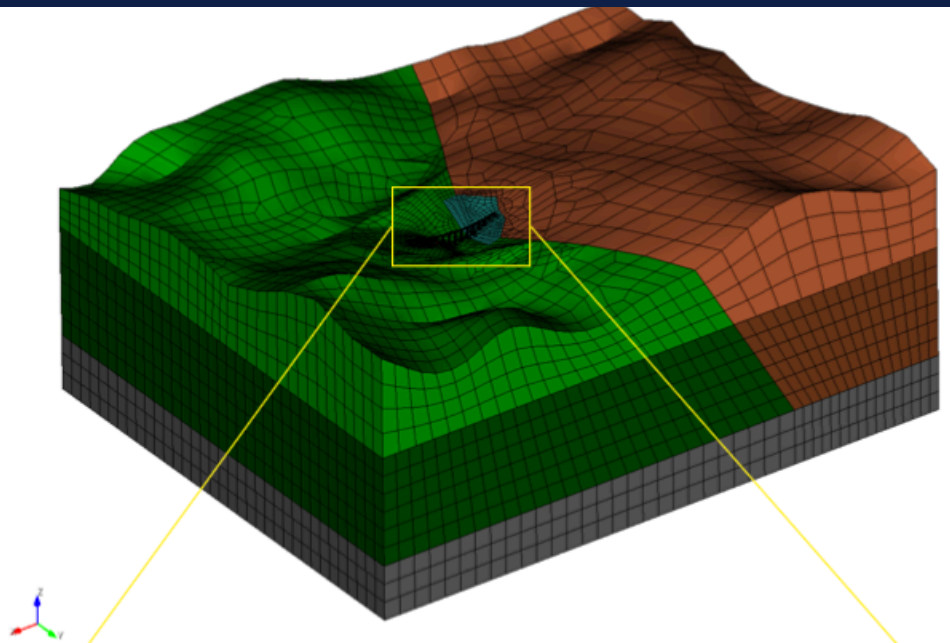

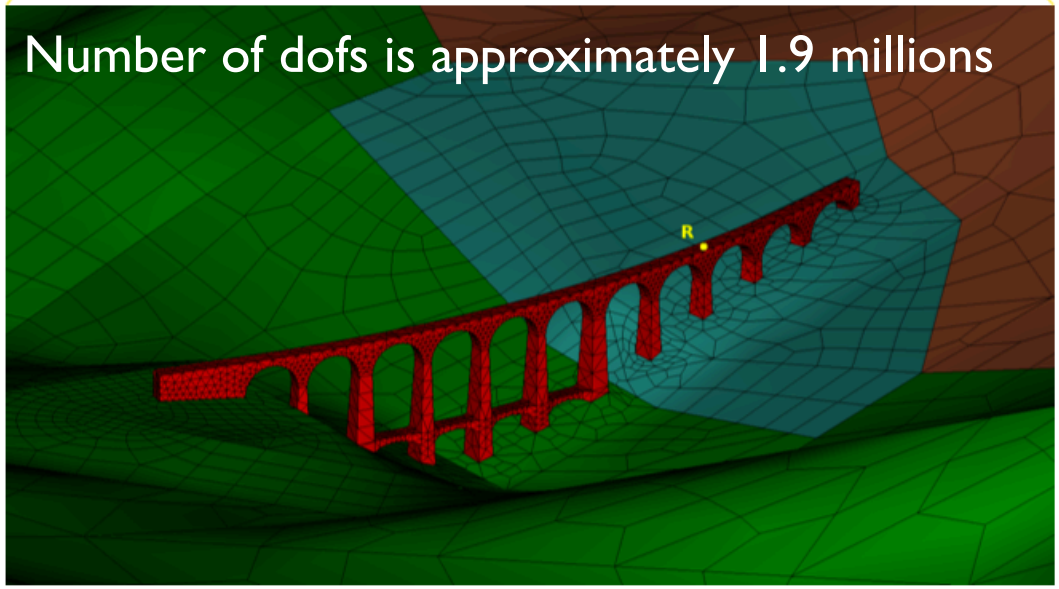


| Material | $\rho[kg/m^3]$ | $c_P$ $[km/s]$ | $c_S$ $[km/s]$ | $Q$ |
|---|---|---|---|---|
| erpentine Jurassic | 2800 \| 2400 | 2.3 \| 1.1 | 1.3 \| 2.4 | 150 \| 125 |
| Calcestic Jurassic | 2800 \| 2500 | 2.3 \| 1.8 | 1.3 \| 2.5 | 150 \| 150 |
| Alluvial basin | 1925 | 0.3 | 0.17 | 25 |
| Bridge | 1750 | 1.22 | 0.72 | 50 |

- Complex topography
- Presence of a vertical subfault that divide the Serpentine and the Calcestic rocks
- Several piers of the bridges rest on a superficial alluvium deposit.
- Broad variability in the spatial scales (hundreds of meters in the geological region — centimeters in the bridge)
- Seismic source: double couple point located at (100,0,−300)m

# Acquasanta Railway bridge, Liguria, Italy

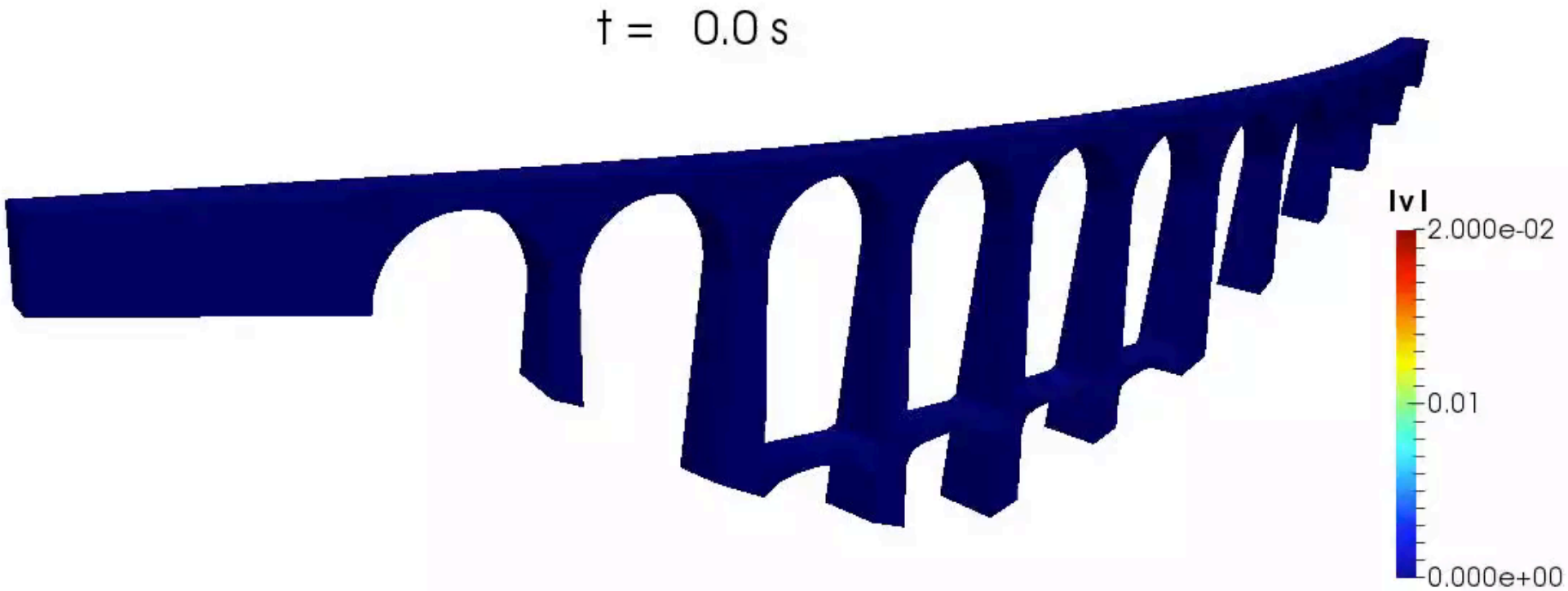


In collaboration with DICA (Politecnico di Milano)

# Christ Church, New Zealand

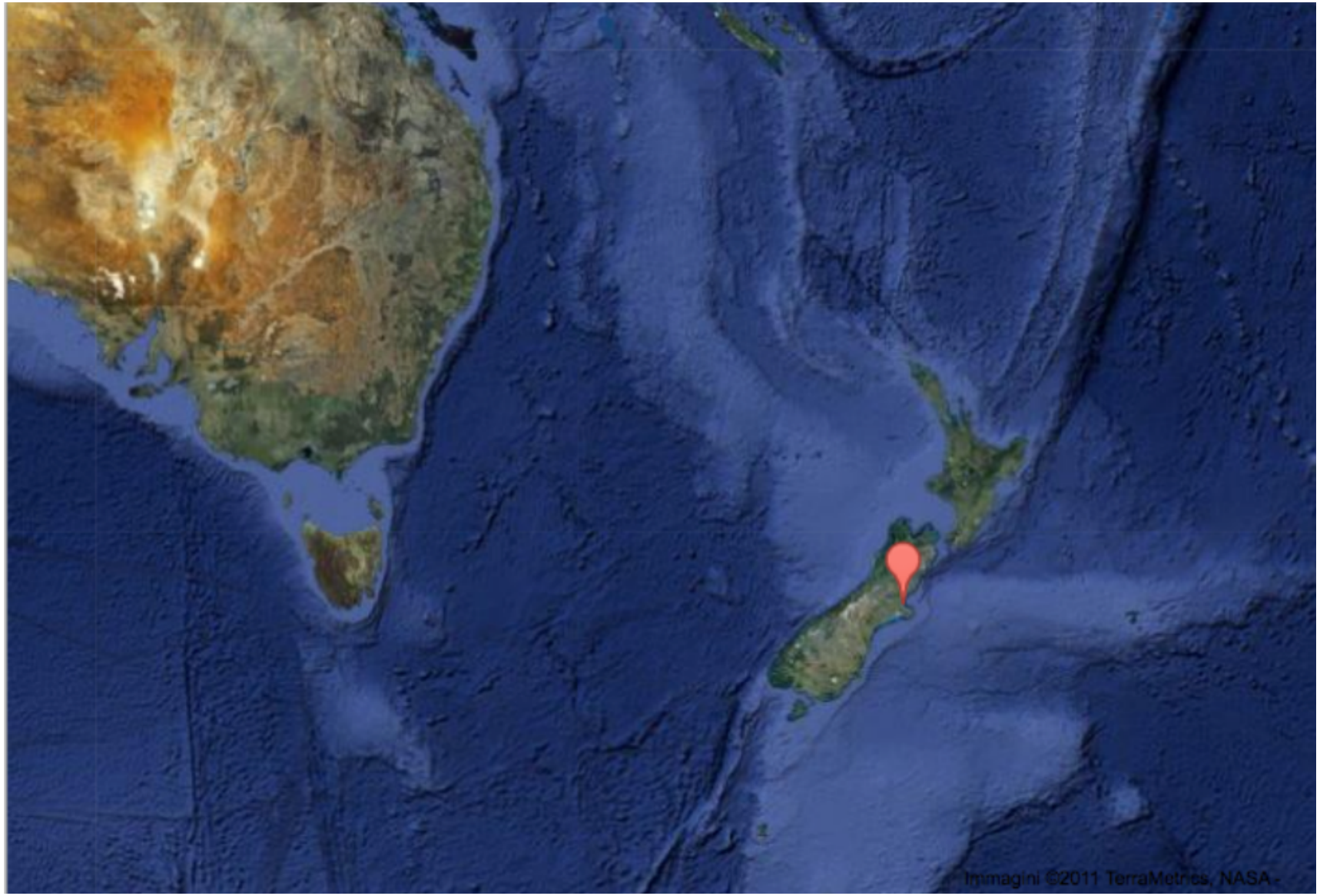


Christ Church, New Zealand ( 22 February 2011)

In collaboration with DICA (Politecnico di Milano)

# Christchurch Central Business District: site-city interaction effects

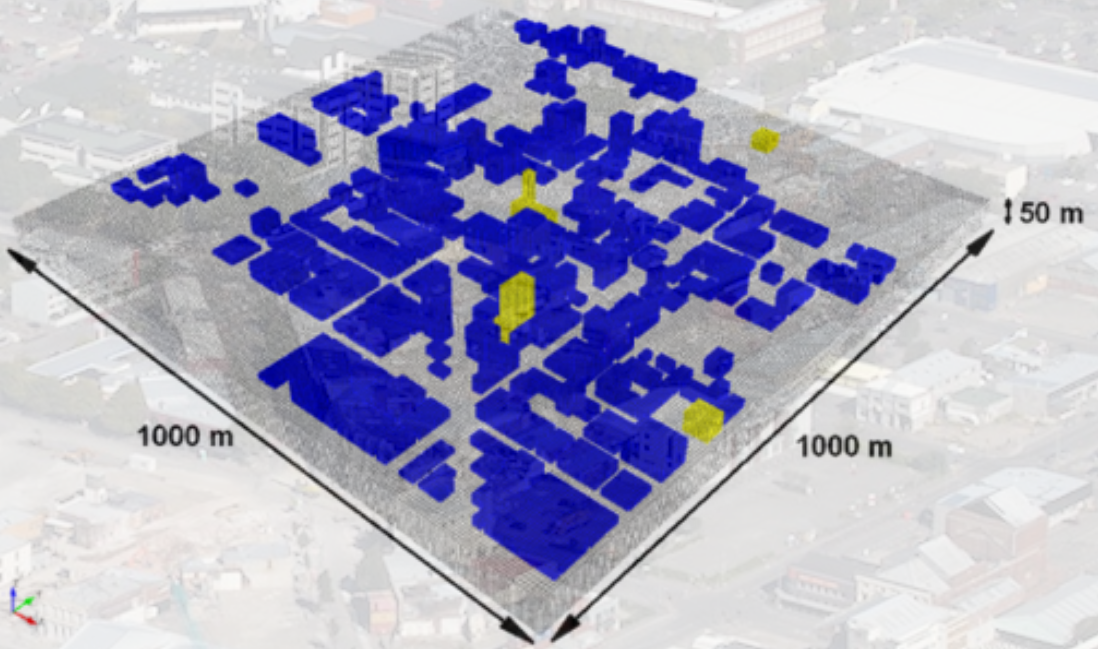


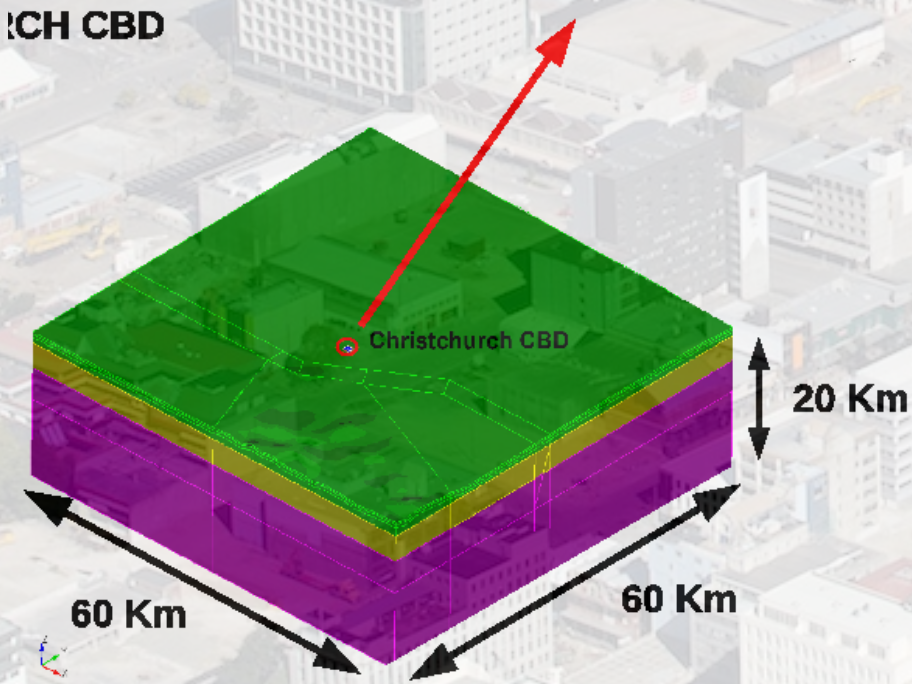


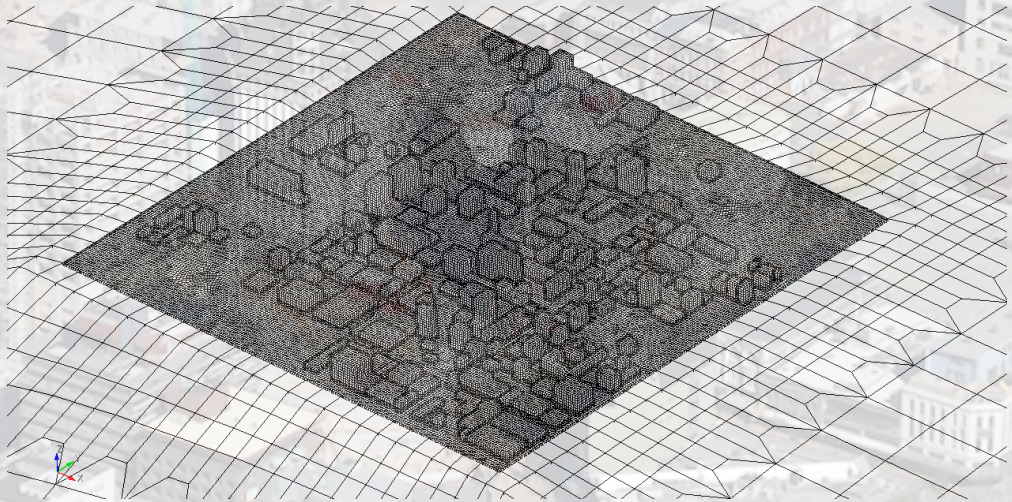


|displ|
100
88.889
77.778
66.666
55.555
44.444
33.333
22.221
11.11
0
z
x
y
step 0
Contour Fill of displ, |displ|.
Deformation ( x0.05): displ of TIME ANALYSIS, step 0.

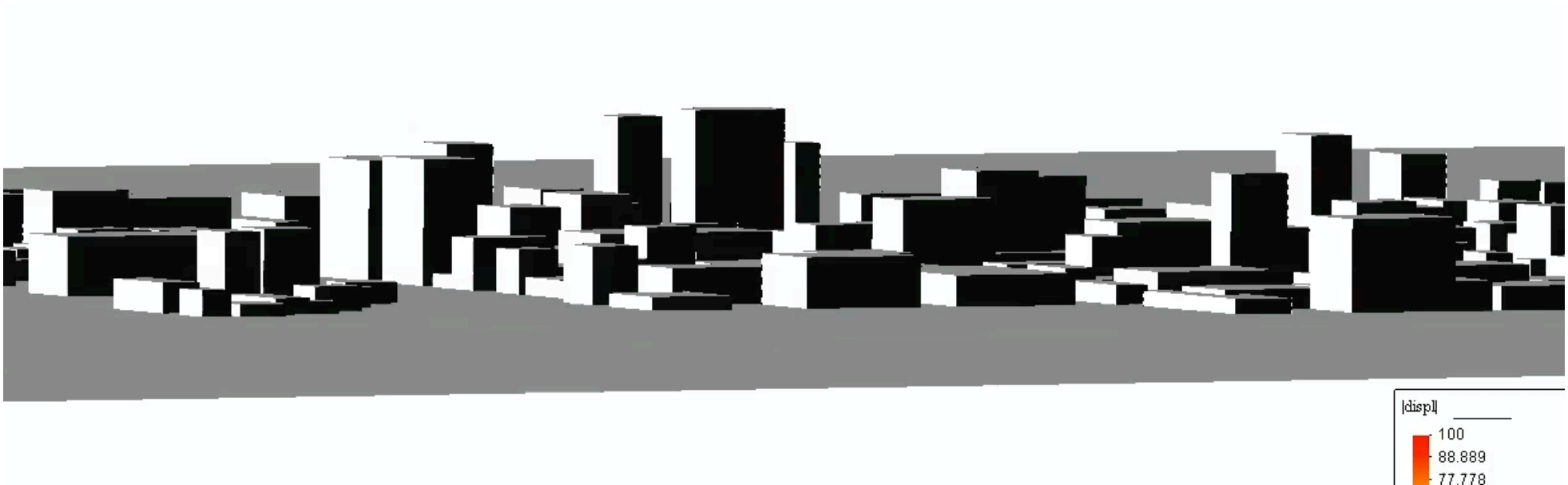
|displ|
100
88.889
77.778


# Emilia earthquake
# 29.05.2012, $M_W$ 6.0

Courtesy of G. Penna

# Emilia earthquake, 29.05.2012, $M_W$ 6.0

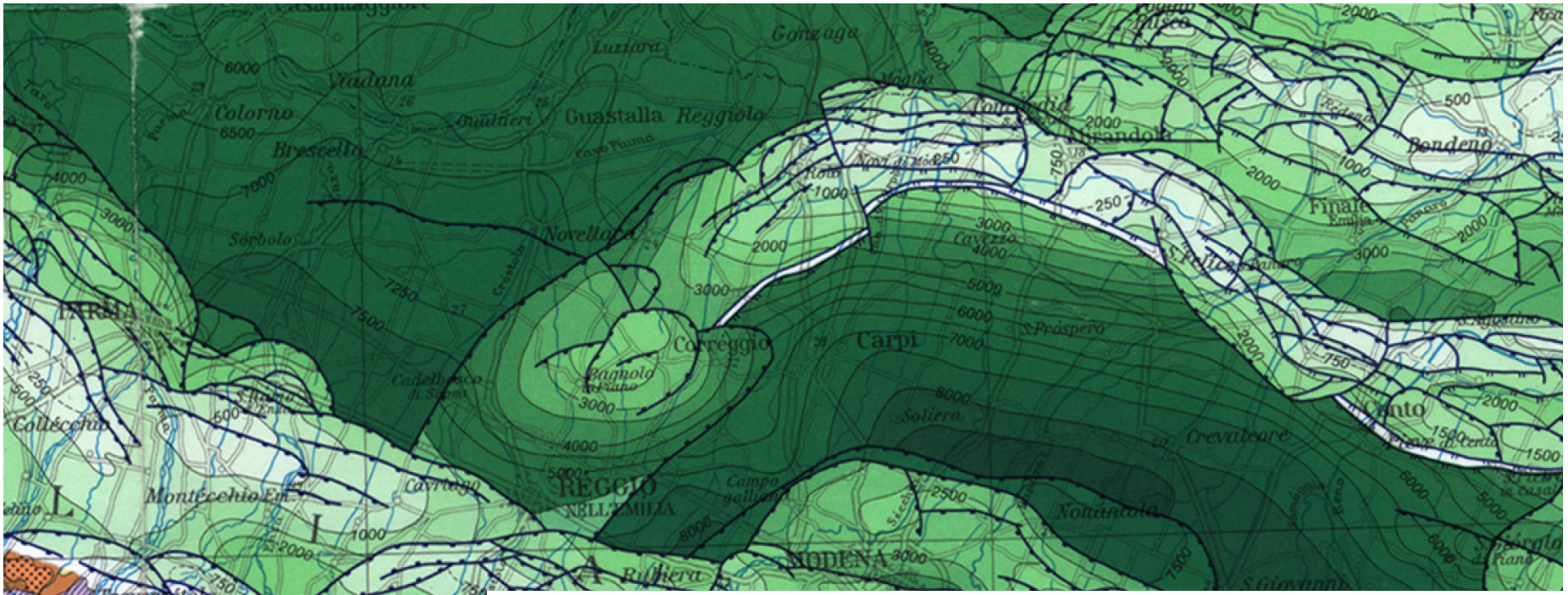


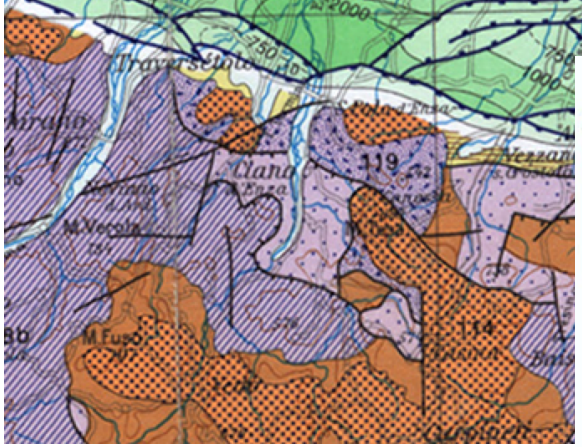


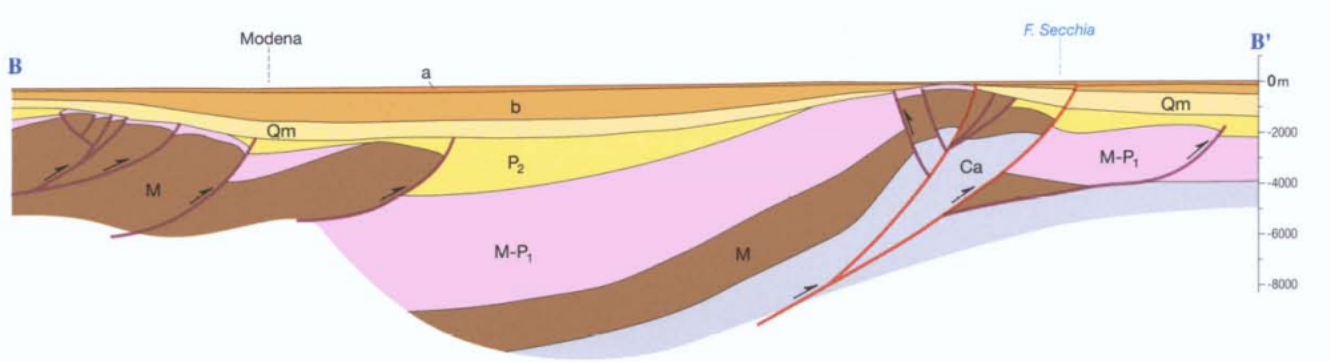


a — Pleistocene medio - Olocene (0,45 Ma-Presente) / *Middle Pleistocene - Holocene (0,45 My-Present)*

b — Pleistocene medio (1 - 0,45 Ma) / *Middle Pleistocene (1 - 0,45 My)*

Qm — Pleistocene inferiore (1,8 - 1 Ma) / *Early Pleistocene (1,8 - 1 My)*

$P_2$ — Pliocene medio-superiore (4,1 - 1,8 Ma) / *Middle-Late Pliocene (4,1 - 1,8 My)*

L — Unità Liguri, Subliguri ed Epiliguri (205 - 6,8 Ma) / *Ligurian, Subligurian and Epiligurian Units (205 - 6,8 My)*

$M-P_1$ — Messiniano sup. - Pliocene inf. (6,3 - 4,1 Ma) / *Late Messinian-Early Pliocene (6,3 - 4,1 My)*

E — Evaporiti messiniane (6,8 - 6,3 Ma) / *Messinian Evaporites (6,8 - 6,3 My)*

M — Miocene (24 - 5,4 Ma) / *Miocene (24 - 5,4 My)*

Ca — Successione carbonatica meso-cenozoica (227 - 24 Ma) / *Meso-Cenozoic carbonatic succession (227 - 24 My)*

T — Triassico inferiore e medio (250 - 227 Ma) / *Lower and Middle Triassic (250 - 227 My)*

# Emilia earthquake, 29.05.2012, $M_W$ 6.0

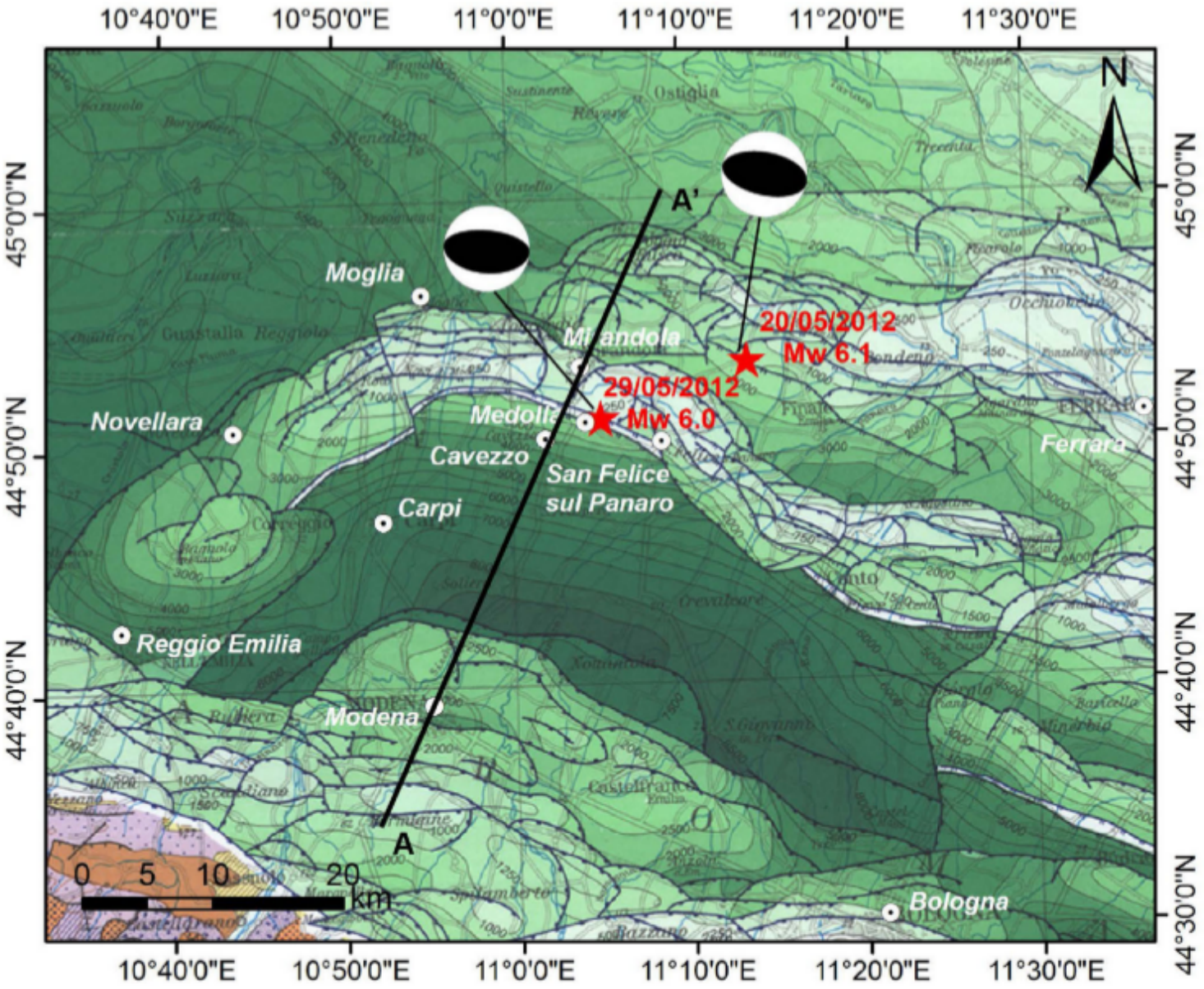


Epicenter areas of the main shock 20.05 ($M_W$ 6.1) and 29.05 ($M_W$ 6.0).

# Emilia earthquake, 29.05.2012, $M_W$ 6.0

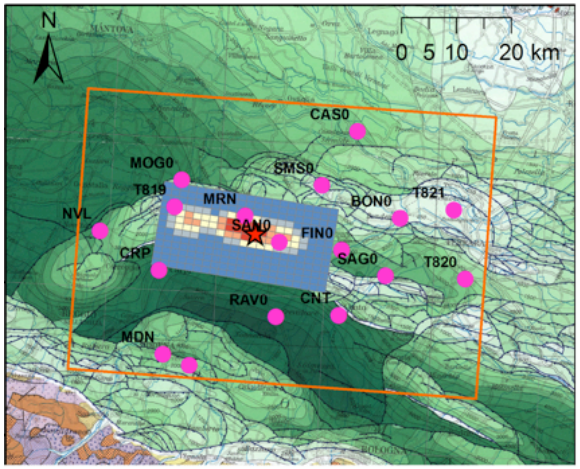


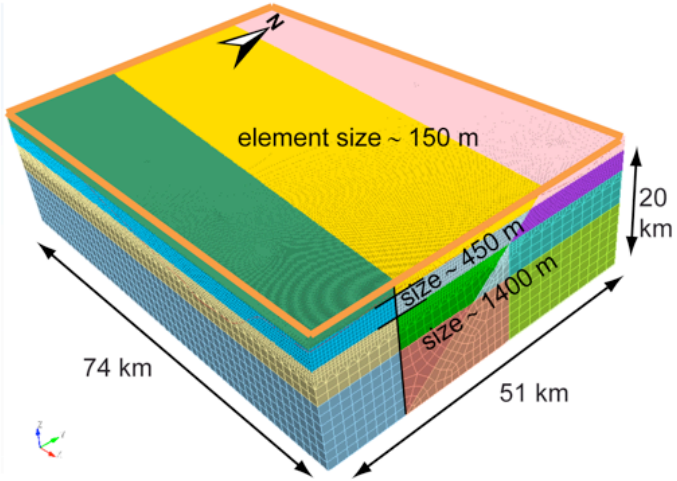


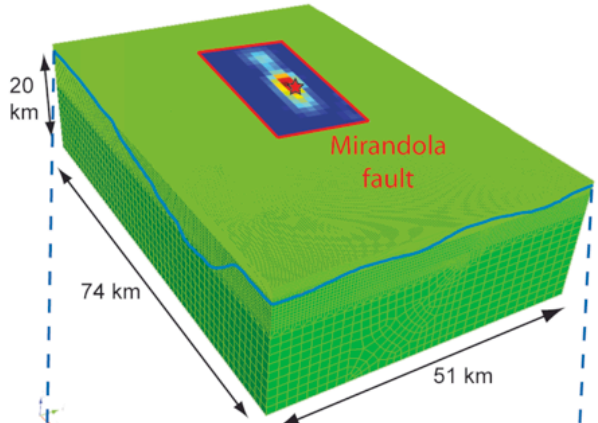


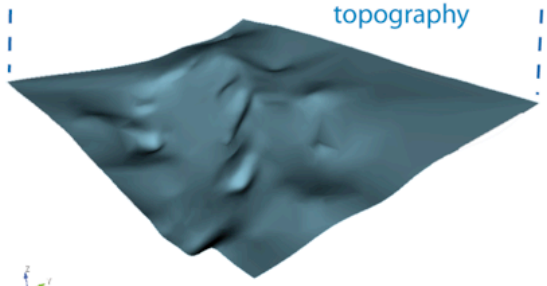


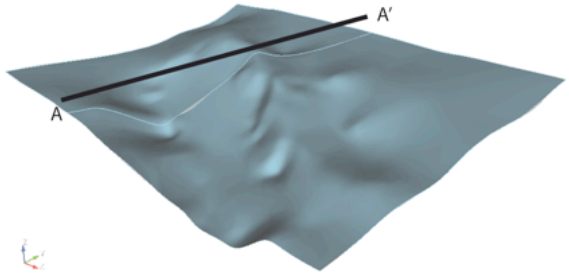


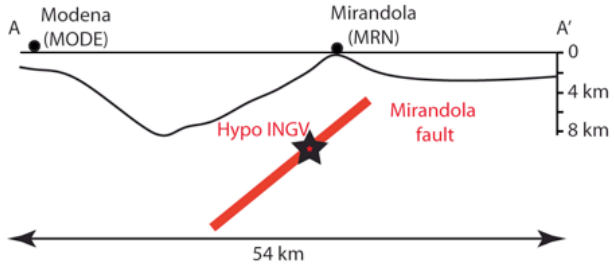


Number of dofs is approximately 150 millions

# Validation of numerical results

Comparison between recorded (black) and simulated seismograms.
12 selected stations, three components of the velocity.

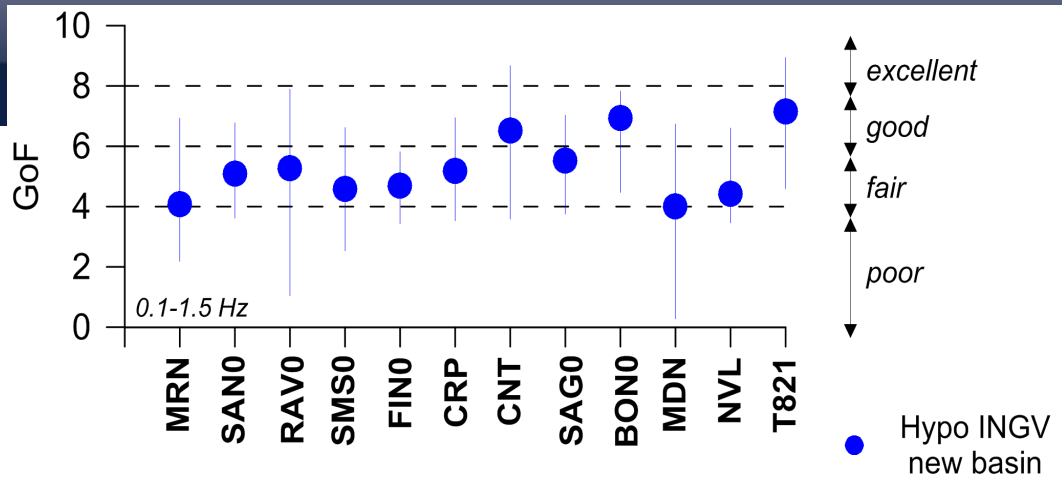


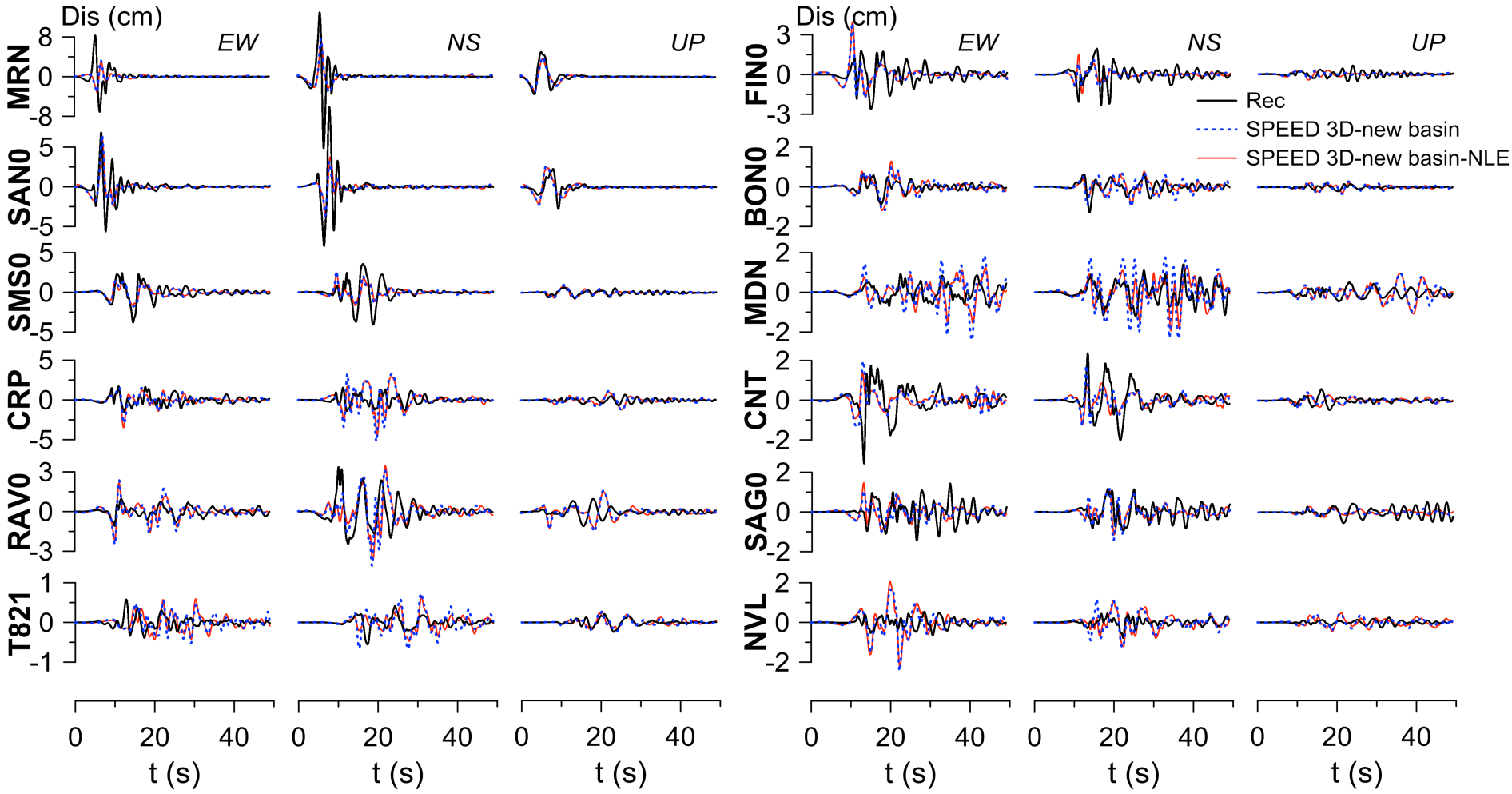

# Comparison with satellite data

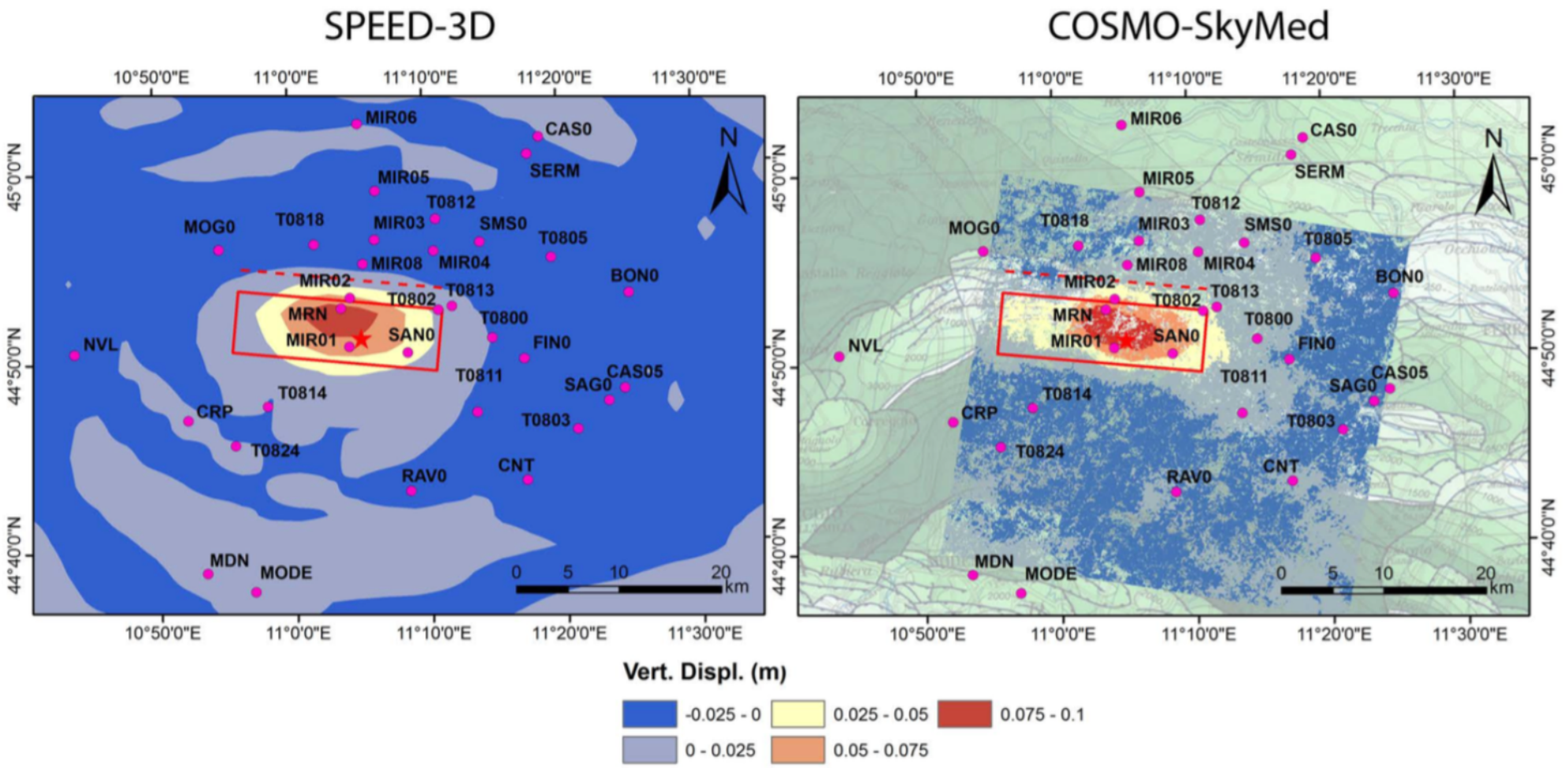


Map of permanent ground uplift simulated by SPEED (left) and observed by COSMO-Skymed InSAR processing (right)

Good agreement between simulated and observed satellite data

# Istanbul case study

# Istanbul case study

Computational domain of the Istanbul region adopted in the present work. Fault system (CMB and NBF) included in the domain as well as topography and bathymetry model

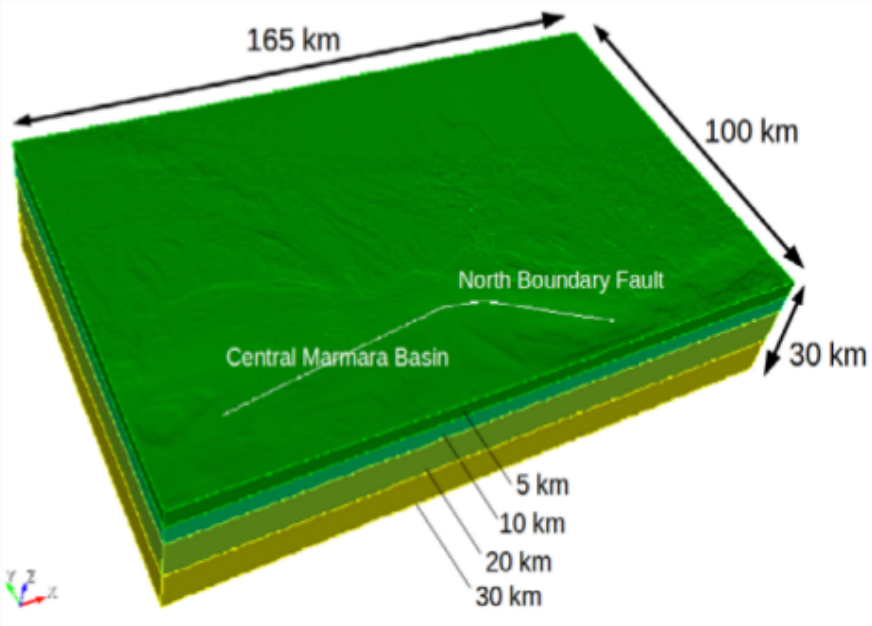


fmax = 1.5 - 2 Hz
hexahedral elements = 2,257,482
degrees of freedom = 475 million
Min. element size = 180 m
Max. element size = 600 m (at 2 km depth)

VS,30 classes defined according to Özgül, 2011.

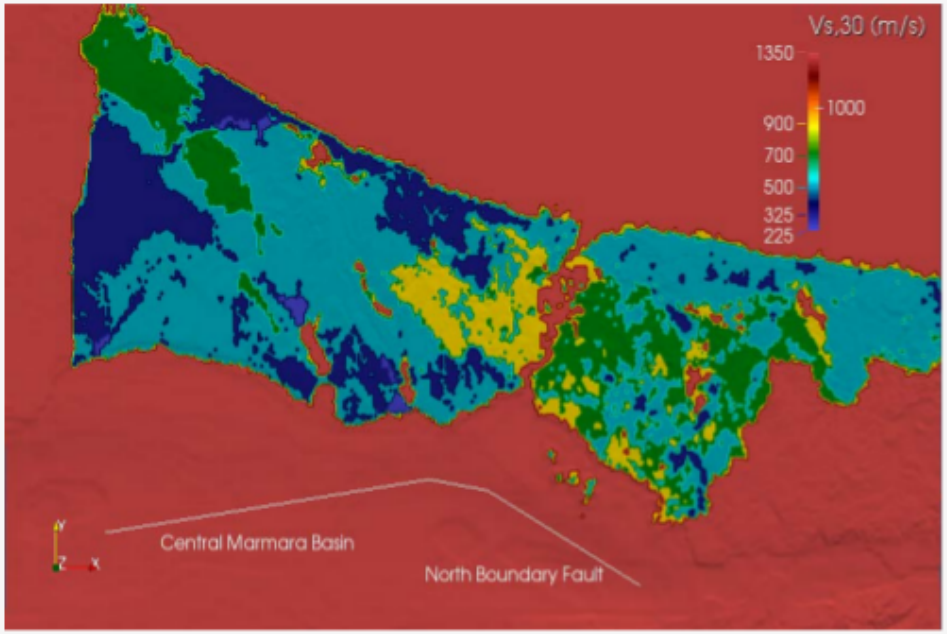


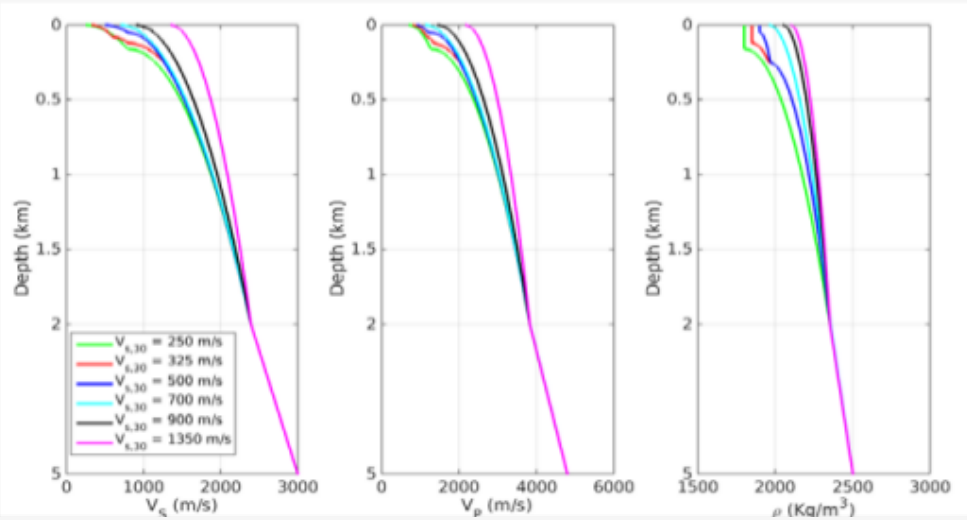

# The case study: Istanbul




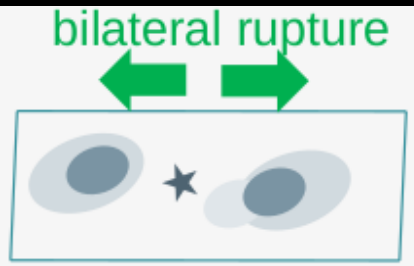


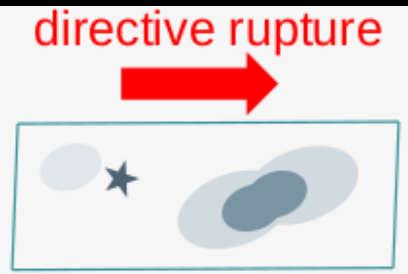


# Grazie